Available online at www.sciencedirect.com
ScienceDirect
Tetrahedron 63 (2007) 7334–7348
Tetrahedron

Molecular mechanism of physical gelation of hydrocarbons by fatty acid amides of natural amino acids

Asish Pal, Yamuna K. Ghosh and Santanu Bhattacharya*

Department of Organic Chemistry, Indian Institute of Science, Bangalore 560 012, Karnataka, India

Received 30 October 2006; revised 19 March 2007; accepted 4 May 2007
Available online 22 May 2007

Abstract—A variety of fatty acid amides of different naturally occurring L-amino acids have been synthesized and they are found to form gels with various hydrocarbons. The gelation properties of these compounds were studied by a number of physical methods including FTIR spectroscopy, X-ray diffraction, scanning electron microscopy, differential scanning calorimetry, rheology, and it was found that gelation depended critically on the fatty acid chain length and the nature of the amino acid. Among them L-alanine based gelators were found to be the most efficient and versatile gelators as they self-assemble into a layered structure to form the gel network. Mechanisms for the assembly and formation of gels from these molecules are discussed.

1. Introduction

The gelation of organic solvents by a diverse group of small molecules is a fascinating phenomenon, which involves molecular self-assembly.[1] The supramolecular association of these low-molecular-mass organogelator (LMOG) leads to physical gel formation, which represents macroscopic expression of their self-assembly via various non-covalent interactions.[2] These nanostructured materials are not only of academic interest but also offer potential application in industrial fields such as cosmetics, food, medical science, tissue engineering, etc.[3] Such LMOGs include a wide variety of molecular structures such as long chain hydrocarbons,[4] amino acid derivatives,[5] carbohydrate derived systems,[6] dendrimers,[7] steroid derivatives,[8] metal complexes,[9] and even two component systems.[10] Other types of amphiphilic molecules have also been used to achieve gelation of water and/or organic media.[11] Some of the above have been developed by rational molecular design and some have been discovered serendipitously. However, it has been recognized that an effective gelator should possess functional groups that interact with each other via temporal associative interactions. This is because an organogelator generally relies on its ability to self-assemble via non-covalent interactions including hydrogen bonding.[12]

Organogelators are generally not capable of gelating organic solvents in the presence of water because water competes for the hydrogen bonding sites in the gelator. Oil spills and toxic solvent-based industrial effluents are major offenders of the ecological balance and the environment. By transforming the 'offending' oil or toxic organic solvent into a solid-like gel, containment of the spill, concomitant removal of the separated 'solid' from the affected water body, and subsequent retrieval of the spilt oil or solvent may all be accomplished. To alleviate these situations involving oil spills, it is necessary to selectively gelate oil in presence of large quantities of water. We have previously reported that fatty acid amides of L-alanine **2c** can gelate oil selectively from oil–water mixtures.[13] Since then, several reports have appeared in literature that addresses this important problem of phase selective gelation.[14] However, the fatty acid amides of amino acid system that were reported by us have one important advantage in that these molecules are totally biocompatible[15] and hence biodegradable. Recently, we have shown that the cavities inside such gel networks can encapsulate different kinds of nanoparticles to give rise to novel nanocomposites with new properties.[16] The LMOG network can also be used as template to synthesize nanostructured materials.[5c,17] Thus, on one hand, a broad variety of molecular structures are available that form gels under appropriate conditions. At the same time it is still challenging to design and synthesize specific gelators especially for a given application. Whatever may be the case, gelators based on biocompatible molecules are of particular importance in that they do not contribute any environmental hazard. To design new gelators based on biocompatible frameworks for various applications, a detailed molecular level understanding of this kind of LMOGs is necessary. In the present work, we have synthesized a large number of fatty acid amides of different amino acids (Chart 1) that are related to **2c**. We have now

Keywords: LMOG; Self-assembly; Organogels; Viscoelastic materials; Layered structures.
* Corresponding author. Tel.: +91 80 2293 2664; fax +91 80 2360 0529; e-mail: sb@orgchem.iisc.ernet.in

0040–4020/$ - see front matter © 2007 Elsevier Ltd. All rights reserved.
doi:10.1016/j.tet.2007.05.028

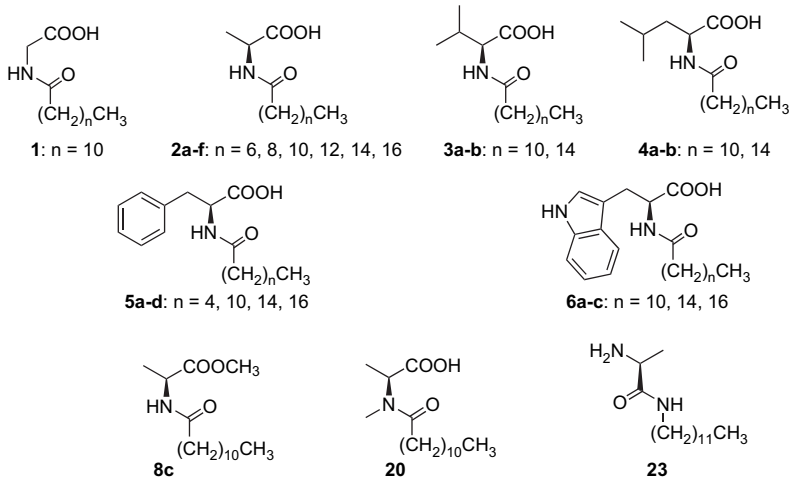

Chart 1. Molecular structures of various fatty acid amides of different amino acids.

carefully investigated the various molecular features that might be responsible for the onset of gelation. Based on this study, we have proposed a molecular mechanism that might be useful for the design of this class of LMOGs for specific applications.

2. Results and discussion

We have been interested in designing amphiphilic molecules that are based on natural components as they are biodegradable and self-assemble in organic solvents to form gels. Toward this end, we considered suitable *N*-acyl-L-amino acid derivatives. In order to understand the mechanism of gelation as well as to determine the minimal structural motifs required by these systems to exhibit efficient gelation, a number of such derivatives were considered. First, five *N*-dodecanoyl derivatives of amino acids bearing side chains of differing hydrophobicities were synthesized (Chart 1). These are derivatives of naturally occurring amino acids glycine (**1**), L-alanine (**2**), L-valine (**3**), L-leucine (**4**), L-phenylalanine (**5**), and L-tryptophan (**6**). Compound **1** does not possess chirality while compounds **2–6** are all chiral. Compound **2** has a CH_3 side chain, **3** has two CH_3 side chains, and **4** has an isopropyl side chain. However, **5** and **6** differ from the rest in that they have aromatic side chains. In order to probe the role of the lipophilic segment in determining gelation properties, fatty acid derivatives of the above molecules with different chain lengths were also synthesized (Chart 1).

To investigate the role of the various functional units in such *N*-acyl-L-amino acid derivatives toward gelation, **2c** was chosen (Chart 1). Compound **8c** was prepared where the CO_2H group in **2c** was converted to the corresponding methyl ester to probe the role of the CO_2H moiety in gelation. Similarly, the secondary –NH–CO– linkage between the lauroyl chain and the alanine unit in **2c** was modified to the corresponding tertiary amide –N(CH_3)–CO– (as in **20**) to examine the importance of this linkage toward self-assembly of **2c**, a pre-requisite of gelation. A derivative **23** was synthesized, where the amine residue in L-alanine was left free and the lipophilic chain was introduced via an amide linkage to the –CO_2H end.

2.1. Synthesis

The syntheses of all the lipophilic amino acid derivatives **1–6** were easily accomplished in high yields using one or two step procedures as summarized in Schemes 1–3. The methyl ester hydrochlorides of individual amino acids were acylated with the appropriate fatty acid chloride in dry $CHCl_3$ in the presence of 2 equiv of Et_3N. The individual *N*-acyl amino acid methyl ester was then carefully hydrolyzed with 1 M NaOH (2 mL) in MeOH/THF (5:1) as shown in Scheme 1. Similarly, the *N*-acyl derivatives of L-amino acids of various chain lengths were synthesized taking the aliphatic acid of desired chain length. Another derivative, *N*-methyl-L-alanine was converted to its *N*-lauroyl derivative (**20**) in good yield and high purity as shown in Scheme 2. For the synthesis of **23**, *N*-benzyloxy-L-alanine was first converted to the corresponding amide by DCC coupling using *n*-dodecylamine. Removal of the *N*-protecting group in **22** by hydrogenation in the presence of 10% Pd/C yielded **23** as shown in Scheme 3. All the compounds isolated were characterized adequately by analytical and spectroscopic means and the corresponding data were consistent with their given structures (cf. Section 4).

2.2. Gelation properties

Gelation of each of the compounds **1–6** was tested by dissolution of 10 mg of each new compound individually by heating in a given solvent (1 mL). Upon cooling to room temperature and inversion of the vial, if the solution did not flow out of the vial, the compound was judged to be a gelator of the corresponding solvent. Here the gelation numbers of the gelators represent the maximum number of solvent molecules that get entrapped per molecule of the gelators.

The abilities of aliphatic amino acid based molecules, **1–4**, to gelate aromatic hydrocarbon solvents like toluene and aliphatic hydrocarbons like *n*-heptane and *n*-hexane were checked initially (Table 1). Interestingly, **1** did not show gelation in any hydrocarbon and this can be attributed to the lack of chirality in the molecule. The L-alanine based molecules formed nice transparent and stable gels from various aromatic hydrocarbons such as toluene, benzene, xylene,

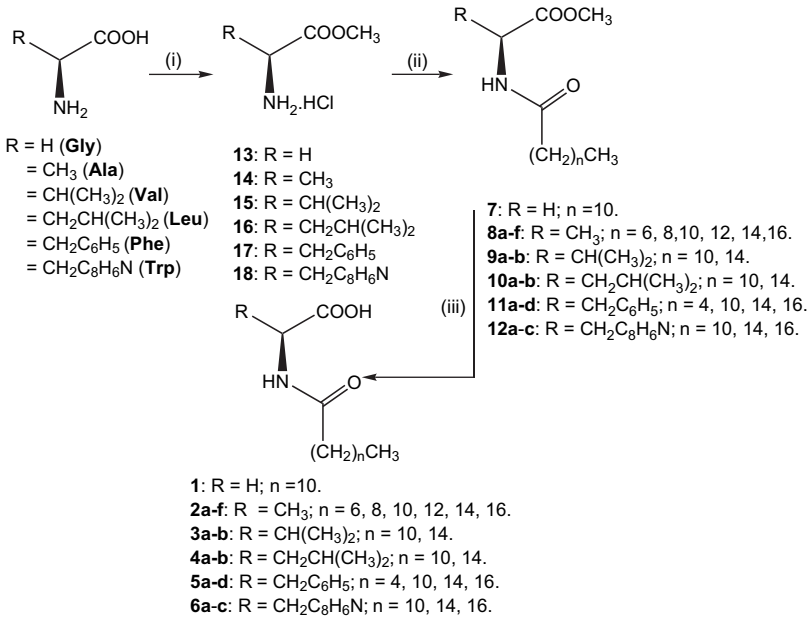

Scheme 1. *Reagents, conditions, and yields*: (i) $SOCl_2$, dry MeOH, 6 h, 99%. (ii) (a) 1 equiv $KHCO_3/H_2O$; (b) *n*-$CH_3(CH_2)_nCOCl$, dry $CHCl_3$, Et_3N (2 equiv), 0 °C, 5 h (**7**=94%, **8a**=93%, **8b**=90%, **8c**=97%, **8d**=94%, **8e**=93%, **8f**=95%, **9a**=91%, **9b**=93%, **10a**=81%, **10b**=88%, **11a**=72%, **11b**=83%, **11c**=74%, **11d**=76%, **12a**=83%, **12b**=80%, **12c**=82%). (iii) (a) MeOH/THF, NaOH/H_2O, 2 h; (b) 0 °C, HCl/H_2O (**1**=98%, **2a**=98%, **2b**=93%, **2c**=97%, **2d**=95%, **2e**=94%, **2f**=92%, **3a**=90%, **3b**=93%, **4a**=98%, **4b**=91%, **5a**=78%, **5b**=98%, **5c**=95%, **5d**=93%, **6a**=98%, **6b**=91%, **6c**=88%).

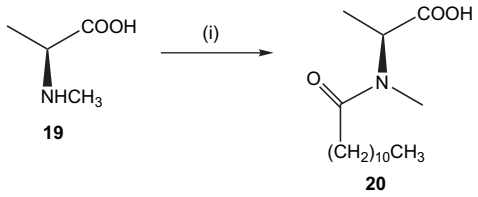

Scheme 2. *Reagents, conditions, and yields*: (i) $CH_3(CH_2)_{10}COCl$, dry DMF, Et_3N (1 equiv), 0 °C, 6 h, 64%.

mesitylene, etc. depending on their chain length. Accordingly, modifications of the nature and size of the lipophilic segment of amino acid based gelators were carried out in order to probe the role of this part in gelation. While **2c** and **2d** showed excellent gelation at 25 °C, **2e** and **2f** having C16 and C18 chains, respectively, could only form weak gels. From Figure 1 it is evident that an optimum lipophilic long chain is very important for forming good gels and hence the gelation number of toluene gels of **2c** and **2d** decreases with increasing lipophilicity. Again **2b** having a C10 chain could form gels in toluene only at low temperature

Table 1. Gelation ability of fatty acid amides of amino acids in different hydrocarbons at 25 °C

Compound[a]	Toluene	Heptane	Hexane
1	I	I	I
2a	S	S	S
2b	S	G	G
2c	G	G	G
2d	G	G	G
2e	W	W	P
2f	W	P	I
3a	S	A	A
3b	S	A	A
4a	S	P	P
4b	S	A	A
5a	S	I	I
5b	S	A	A
5c	S	G	G
5d	S	W	W
6a	S	I	I
6b	S	I	I
6c	S	I	I

[a] Gelator of 1 wt % was used for all tests; G: good gel, S: sol, I: insoluble, P: immediate precipitation, A: aggregation leading to gradual precipitation, W: weak gel.

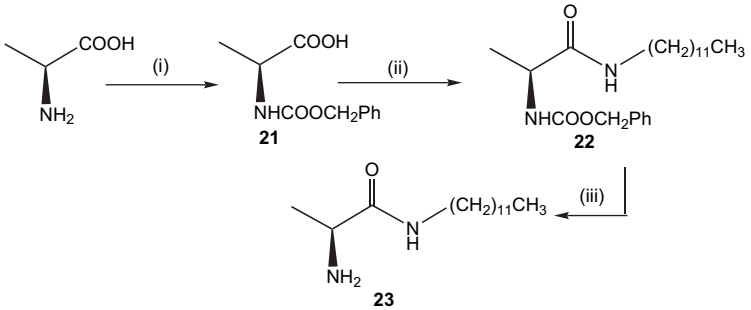

Scheme 3. *Reagents, conditions, and yields*: (i) $PhCH_2OCOCl$, NaOH/H_2O, 0 °C, 2 h, 72%. (ii) *n*-$CH_3(CH_2)_{11}NH_2$, DCC, dry THF, rt, 24 h, 78%. (iii) 10% Pd/C, H_2, 10 h, 87%.

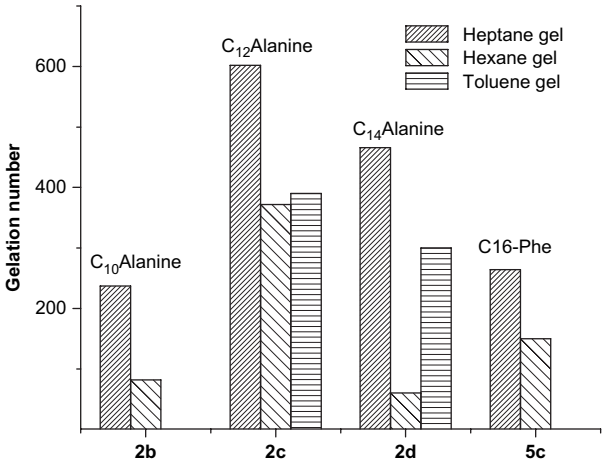

Figure 1. Bar diagram showing gelation numbers of **2b**–**2d** and **5c** in toluene, hexane, and heptane.

(<20 °C) and **2a** having a short C8 chain did not show any observable gelation even at low temperatures (up to ~4 °C).

For aliphatic hydrocarbons like *n*-heptane and *n*-hexane, gel formation was restricted to **2b**–**2d** among the L-alanine derivatives having C10, C12, and C14 chain lengths, respectively. Figure 1 shows that the gelation number of the gels in *n*-heptane and *n*-hexane was also dependent on the lipophilicity of the gelator molecules and was highest for **2c** with a C10 chain.

Notably, the fatty acid amides of racemic alanine did not gelate any hydrocarbon solvent irrespective of their chain lengths. In contrast, individual fatty acid amides of both D- and L-alanine showed efficient gelation in both aromatic and aliphatic solvents. This suggests that chirality is an important determinant for gelation by this class of materials.

Interestingly, replacing L-alanine in these compounds with L-valine and L-leucine also virtually abolished the gelation properties. The derivatives of these two amino acids were completely soluble in toluene, but in *n*-heptane and *n*-hexane they formed aggregates (note that precipitates formed immediately after cooling the solution but aggregates formation took longer time). These aggregates are not efficient enough to entrap many solvent molecules as required for good gelation and hence gelation number could not be accurately determined. Increasing the lipophilicity and steric bulk near the chiral carbon center therefore inhibited the resulting fatty acid amides from forming efficient gel networks.

For aromatic amino acids, e.g., L-phenylalanine and L-tryptophan based molecules, their high solubilities in toluene ruled out gelation in aromatic solvents. However, in aliphatic hydrocarbons, e.g., in *n*-heptane or *n*-hexane, gelation was evident depending on the length of the fatty acid chain (Table 1). While **5c** showed gelation in *n*-heptane and *n*-hexane, the shorter chain versions of L-phenylalanine formed 'clumped aggregates' rather than gels. The gelation numbers of the *n*-heptane and *n*-hexane gels of L-phenylalanine derivative **5c** were less than that of the corresponding L-alanine derivative **2c** as evident from Figure 1. Again increasing the chain length above an optimum lipophilicity, as in **5d**, made the gel weaker. L-Tryptophan based molecules were mostly insoluble in the aliphatic solvents.

The kinetics of gelation were interestingly different depending on the nature of the amino acid side chain and the length of the fatty acid chain as well as the solvent molecules in which the compound is gelated. For aliphatic amino acid based gelators, the onset of gelation in *n*-heptane and *n*-hexane was very fast and was complete immediately upon reaching the room temperature (~1–2 min). In contrast, in aromatic hydrocarbon like toluene the gelation process was slower and was complete within 10 min at ambient temperature. For the gelators possessing amino acids with aromatic side chains, the time required for gelation was much longer (nearly 1 h). The slower kinetics of gelation for the gelators with aromatic side chains, or in aromatic hydrocarbon solvents, are presumably due to the bulky nature of the side chain residues relative to that in aliphatic gelators or in aliphatic hydrocarbons (see below). In addition, in aliphatic hydrocarbon solvents, it is possible that the fatty acid chain of the gelators could mix easily to facilitate the process of self-assembly leading to gelation. It appears that in order to generate the optimized three-dimensional arrangement of the aromatic molecules necessary for gelation, the flat aromatic side chain residues position themselves for π-stacking interactions, which takes a longer time to attain. Since there is no possibility of achieving such stabilization for **3** and **4**, the isopropyl and isobutyl groups only create steric congestion leading to inefficient gelation. However, since the methyl group in **2** is quite small, the self-association is much faster. Interestingly, **1** was unable to gelate any solvent due to the lack of chirality although the side chain of glycine is the smallest. That chirality is essential for these systems to exhibit gelation is evident from the fact that a racemic form of **2a** failed to gelate any of the solvents.[18]

2.3. Sites involved in self-association: FTIR studies

When the methyl ester **8c**, a compound structurally related to **2c**, was used, no gelation was observed in any of the above solvents. Similarly, N-methylation of the amide moiety in **2c** to give **20** again destroyed the gel-forming property of the former compound. It was therefore evident that the presence of both the carboxylic acid (–CO_2H) residue and the amide (–NHC═O) residue is essential for the continuous self-association of the monomers of **2c** into networks possessing the ability to entrap solvent.

FTIR studies were carried out to understand the roles of the –CO_2H and –NH–C═O residues of **2c** in gelating of non-polar solvents. First, FTIR spectra of **2c** at different concentrations in a transparent gel-forming solvent like benzene and a non-gel forming solvent such as $CHCl_3$ were recorded (Fig. 2A and B). The amide N–H asymmetric stretching in $CHCl_3$ appeared at 3430 cm^{-1} (Fig. 2A), which remained invariant with the increase in gelator concentration. A sample of gel produced in benzene was dried in vacuum and the resulting solid was examined by FTIR as a KBr pellet. The N–H stretch in this sample appeared at 3348 cm^{-1} (Fig. 2A) suggesting the preservation of strong intermolecular hydrogen bonding associations in solid **2c**. At pre-gelating concentrations (c=3 mg/mL) in benzene, the amide N–H asymmetric stretching was found

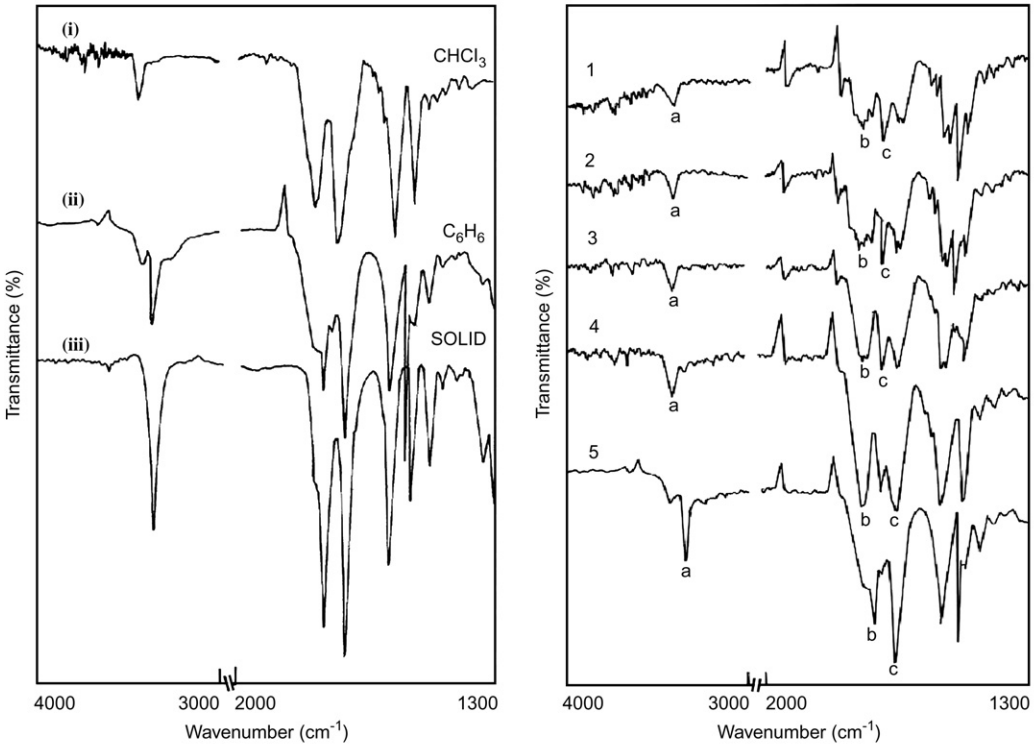

Figure 2. (A) Fourier transform infrared (FTIR) spectra of **2c** in (i) $CHCl_3$ as solution (222 mM), (ii) benzene as solution (222 mM), and (iii) the form of solid. (B) Effect of concentration on the FTIR spectra of **2c** in benzene: (1) 11 mM, (2) 18 mM, (3) 36 mM, (4) 111 mM, (5) 222 mM. The peaks were monitored at (a) 3420–3348 cm^{-1}, (b) 1765–1706 cm^{-1}, (c) 1684–1646 cm^{-1}.

to appear at 3419 cm^{-1}. However, under strongly gelating concentrations (c=60 mg/mL) a major peak appeared at 3348 cm^{-1} at the expense of the signal at 3419 cm^{-1}, which was reduced to a minor peak (Fig. 2B). At $5<c<10$ mg/mL in benzene, the molecules of **2c** are not as strongly associated as in the solid although the presence of intermolecular hydrogen bonding is still evident. This indicates that the solvent molecules do not interfere with the intermolecular association. At identical concentrations in $CHCl_3$ this association is much weaker, as $CHCl_3$ can compete for hydrogen bonding with the individual molecules of **2c**. Strong intermolecular hydrogen bonding in the gel state of benzene is confirmed by the fact that at gelating concentrations of **2c**, this stretch shifts to 3348 cm^{-1} from 3430 cm^{-1}, which is identical to that of the solid non-gelated aggregate.

The *amide I* band at c=3 mg/mL appeared at 1684 cm^{-1} in benzene (Fig. 2B(1)). Increase in c showed the appearance of a hydrogen-bonded species at 1648 cm^{-1}, which became more intense with increase in c and a concomitant decrease in the stretch at 1684 cm^{-1}, almost till its disappearance (Fig. 2B(5)). Notably the *amide I* band in the gel state of **2c** (Fig. 2B(5)) was found to be almost as strongly hydrogen bonded as in the solid aggregate, which showed the corresponding stretch at 1646 cm^{-1}. Note also that in $CHCl_3$ only one stretch for **2c** occurred at 1669 cm^{-1}, which did not vary with concentration (not shown). This could be due to the formation of species where the oxygen of the amide carbonyl is weakly hydrogen bonded to the acidic H of $CHCl_3$. This is confirmed by the fact that **2c** is able to efficiently gelate CCl_4 where the solvent molecules cannot hydrogen bond with **2c**. Thus solvents capable of hydrogen bonding inhibit gelation in these systems by disallowing the continuation of a hydrogen-bonded superstructure formation due to self-assembly of **2c**. On increasing the concentration of **2c** in benzene, the carbonyl band of the CO_2H stretch between 1770 and 1750 cm^{-1} disappeared (Fig. 2B(1)) and a new stretch appeared at 1732 cm^{-1} (Fig. 2B(4)), which could be assigned to the formation of CO_2H dimer. At c=60 mg/mL another stretch appeared at 1706 cm^{-1} (Fig. 2B(5)) suggesting the presence of a strongly hydrogen-bonded network as seen in the solid aggregate (1704 cm^{-1}). However, in $CHCl_3$, **2c** exhibited a stretch at 1750 cm^{-1} at $c<5$ mg/mL. Upon increase in c, this stretch shifted to an intermediate value of 1732 cm^{-1} (not shown).

Taken together these studies show that the gelation by **2c** is caused by the intermolecular hydrogen bonding between the amide linkages (–N–H···(O)=C–N–H···(O)=C–). Such intermolecular association in these systems is significantly affected by the polarity and protic nature of the solvent. The CO_2H sites of **2c** in both $CHCl_3$ and benzene at $c>10$ mg/mL form dimers of comparable strength (1732 cm^{-1}). However, there is a notable difference in the strength of the *amide I* band under similar conditions. It is considerably weaker (1669 cm^{-1}) in $CHCl_3$ than in benzene (1646 cm^{-1}), and it is this difference in strength, which probably determines whether a solvent promotes or inhibits gelation. The dimer formation at the CO_2H end and hydrogen bonding at the amide sites are therefore *both* required for effective gelation. This is reflected in the behavior of

23 where, although the amide link still exists, the free amine cannot associate effectively like the CO_2H moiety and hence gelation does not occur.

2.4. Scanning electron microscopy (SEM)

In order to discern the nature of the microstructures that may be present in such gels with such varying gelation capacity and mechanical strength, we examined the gel samples of alanine based derivatives in toluene and *n*-heptane by scanning electron microscopy. SEM confirmed the presence of fibrous networks in all instances. For the toluene gel of **2b**, **2d**, and **2f**, as the chain length of the lipophilic segment was increased, the thickness of the fiber gradually became larger (Fig. 3A(a–c)). The thickness of fibers was least with **2b** (0.4–0.5 μm), highest with **2f** (2.5–3.5 μm), and intermediate with **2d** (0.5–0.6 μm). For the *n*-heptane gel, a slight variation of fiber dimension was noticed as chain length of the lipophilic part was increased from C10, C12 to C14 (Fig. 3A(d–f)).

The aggregates of the phenylalanine based derivatives in *n*-heptane were also examined through SEM (Fig. 3B). The thickness of fibers was less with **5b** (1–3 μm) but with increased lipophilicity in **5c** the average thickness of the fibers increased to 3.0–4.0 μm. Closer scrutiny reveals that aggregates of L-phenylalanine based gelator show larger pores in the assembly compared to that of L-alanine based gelator.

2.5. Differential scanning calorimetry of the gel

To gain further insights into the thermal stability of the gels, we investigated extensively the thermotropic behavior of the gel prepared in toluene and heptane. The gel-to-sol melting transitions of the individual gel were found to be less sharp than the corresponding freezing transitions from sol to gel. Also, the melting temperatures (T_m) for gel-to-sol were higher than the freezing temperature (T_f) for sol-to-gel transition. This type of hysteresis behavior has also been observed with other gels.[19]

For the toluene gels of L-alanine based gelators of different chain lengths, **2b**–**2f**, both the T_m and T_f were found to increase with increasing chain length (Fig. 4a and Table 2a). Also the value of $\Delta H_{melting}$ for the gel-to-sol transition

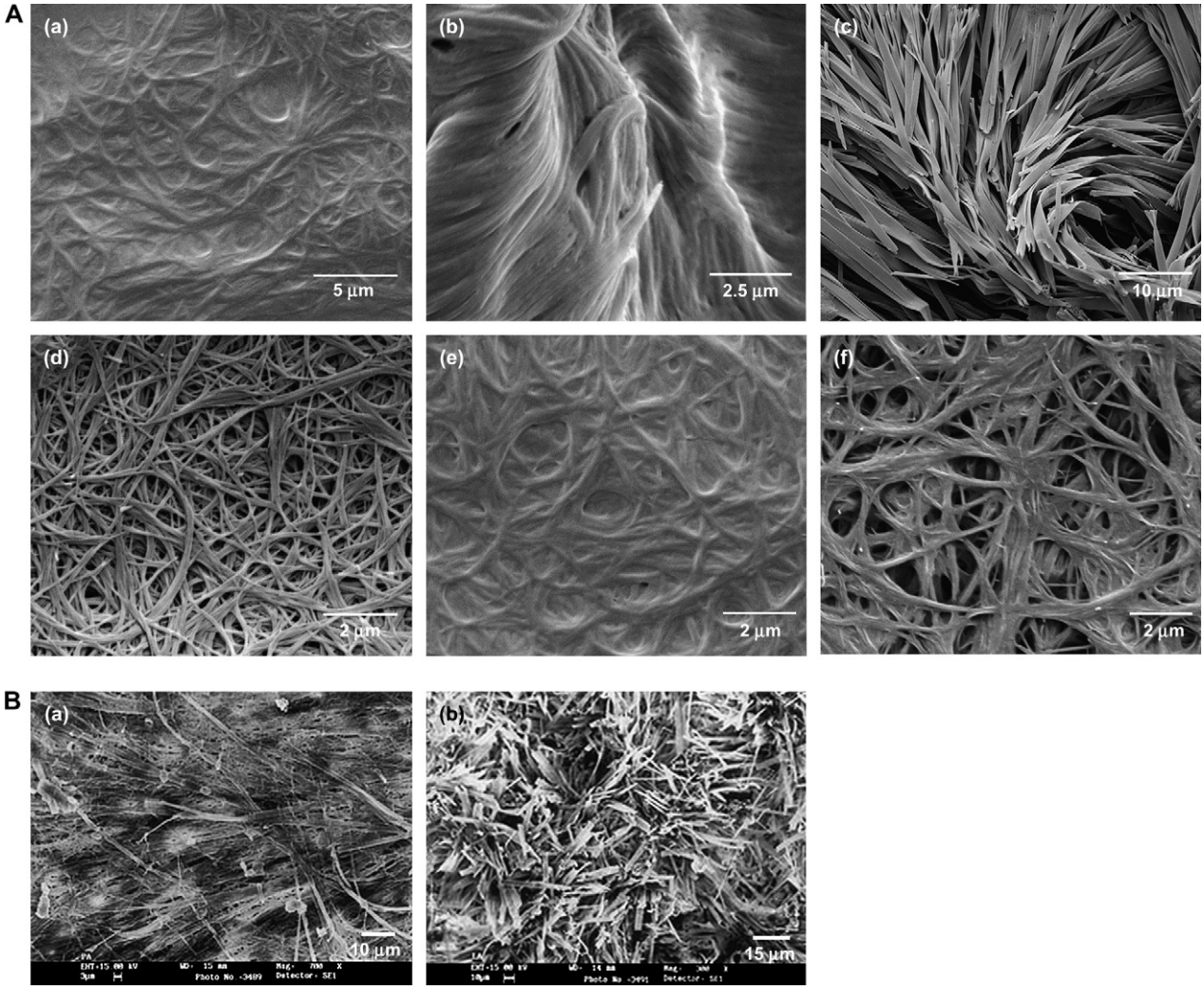

Figure 3. [A] SEM pictures of (a) **2b** in toluene, (b) **2d** in toluene, (c) **2f** in toluene, (d) **2b** in heptane, (e) **2c** in heptane, and (f) **2d** in heptane. [B] SEM pictures of (a) **5b** in heptane and (b) **5c** in heptane.

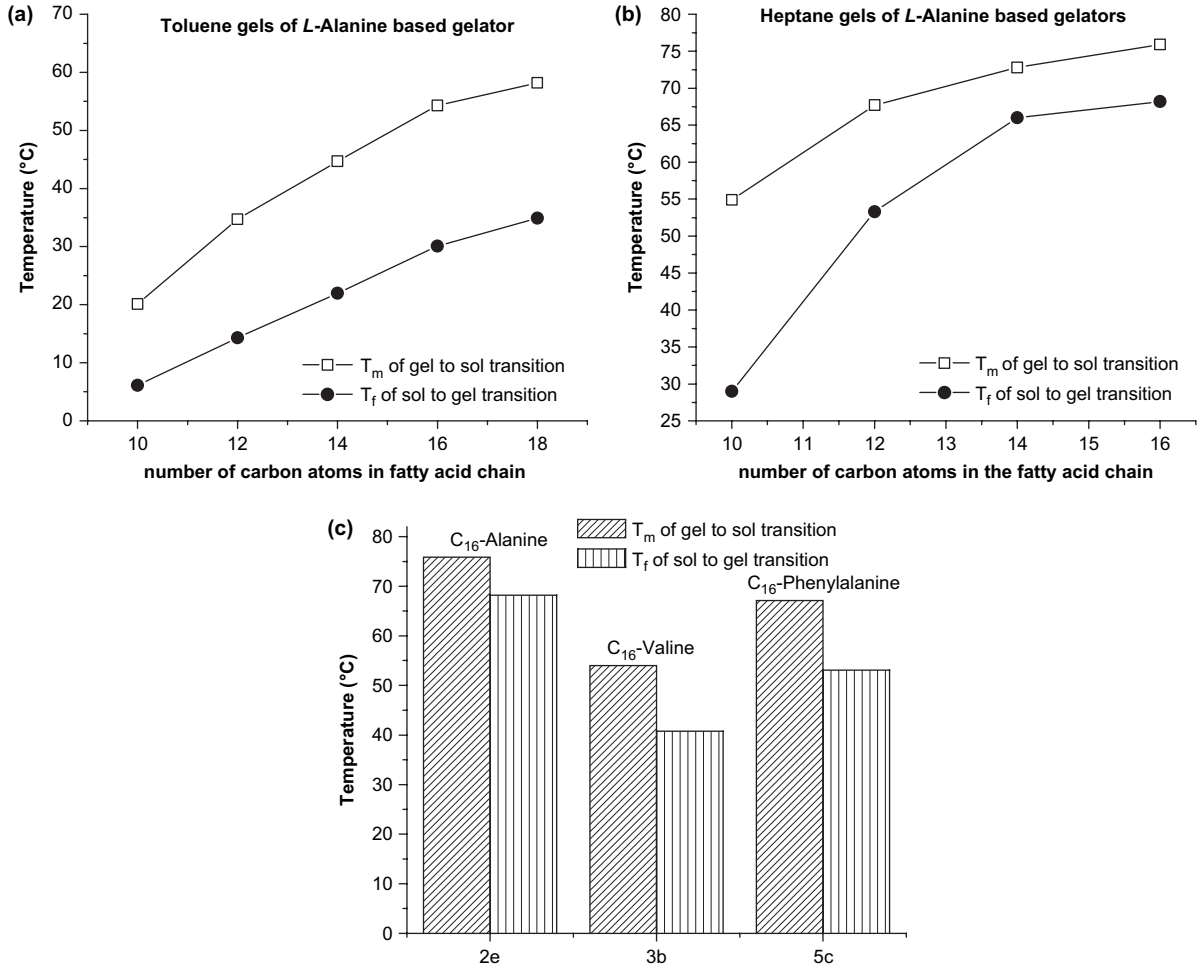

Figure 4. (a) Plot of melting temperature versus number of carbon atoms in the fatty acid chains of L-alanine based gelators for toluene gels. (b) Plot of melting temperature versus number of carbon atoms in the fatty acid chains of L-alanine based gelators for heptane gels. (c) Bar diagram showing the variation of melting temperature for different amino acid gelators. Error in measurement is within ±1 °C.

Table 2. The gel melting temperature from DSC measurement

Gelators[a]	Upscan T_m[b] (°C)	Downscan T_f[b] (°C)
(a) *Toluene gels*		
2b	20.5	6.1
2c	34.7	14.3
2d	44.7	22.0
2e	50.9	29.9
2f	55.9	36.1
(b) *Heptane gels*		
2b	54.8	28.9
2c	67.7	53.2
2d	72.8	66.0
2e	75.9	68.2
3b	54.0	40.8
5c	67.0	53.2

[a] Gelator concentration=10 mg/mL.
[b] Error in the measurement was within ±1 °C.

increased with increasing chain length. This indicates that the van der Waals interactions of the lipophilic portion of the gelator molecules play a significant role in modulating gelation properties endowing the system with thermal stability. Also, heating scan of toluene gels of **2e** and **2f** having C16 and C18 chains gives more than one transition indicating the polymorphic character of the aggregate due to the increase in the chain length. For the *n*-heptane gel of L-alanine based gelators, **2b–2d**, increasing the chain length makes the gelator assembly more thermally rigid (Fig. 4b and Table 2b). Since the *n*-heptane molecules can orient themselves along the lipophilic chain of the gelators, increased chain length endows the gel assembly with more thermal stability. This observation is consistent with the fact that the fiber diameters in these gels increase with the increase in the fatty acid chain length.

To get an insight into the effect of the side chains of the amino acids on the thermal stability of the assembly, palmitoyl chain derivatized gelators of L-alanine (**2e**), L-valine (**3b**), and L-phenylalanine (**5c**) in *n*-heptane were subjected to differential calorimetric analysis. Interestingly, both **3b** and **5c** were thermally less rigid than **2e** (Fig. 4c and Table 2b). This is presumably due to weaker packing among the gelator molecules in the self-assembly as the steric bulk of the side chain hinders the optimal positioning of the individual gelator molecule while forming a three-dimensional network. This explains why replacing L-alanine by any other amino acid makes the gel network significantly weaker. Interestingly, *n*-heptane gel of **5c** is slightly more rigid than that of **3b**, which could be due to the π-stacking interactions that may prevail among the phenyl rings of **5c**. So for aromatic side

chain based gelator **5c**, both steric hindrance and the interaction of the phenyl rings become crucial.

2.6. Rheological studies of the gel

Under applied stress, viscoelastic samples exhibit resistance to flow. The stress versus strain plot yields the complex modulus G^* for the sample, which is the ratio of amplitudes of stress and strain in an oscillatory experiment. G^*, in turn, has two components: (a) G' or the storage modulus, representing the ability of the deformed material to restore its original geometry, and (b) G'' or the loss modulus, representing the tendency of a material to flow under stress. For viscoelastic materials like gels, G' is an order of magnitude greater than G'', demonstrating the dominant elastic behavior of the system. The yield stress (σ_y) refers to the applied stress above which the gel starts to flow—or in other words, changes from a dominant elastic-solid-like behavior to a dominant viscous-liquid like behavior. Usually, this point is determined by measuring the stress value at which G'' becomes larger than G' (in a so-called stress amplitude sweep experiment). Each gel has its own particular σ_y according to its strength or rigidity to an oscillating stress.[20]

The viscoelastic properties of toluene gels with different chain lengths of L-alanine derivative were studied. The yield stress increased remarkably as the lipophilic chain length was increased (Fig. 5). It is very clear that increasing the chain length up to an optimum level makes the gel more viscoelastic. Even for *n*-heptane gels the same trend was observed. As the chain length was changed in the series C10, C12, and C14 the yield stress also increased from 12 to 20 to 40 Pa. Clearly, the increase in the chain length of the fatty acid part in L-alanine compounds enhances the resistance of the gel flow behavior. The *n*-heptane gel of palmitoyl-L-phenylalanine (**5c**) showed a yield stress of 20 Pa, which was even less than that of the C14 derivative of alanine (**2d**). Clearly, the chain lengths of the long acyl chains and the size of the amino acid side chains both determine the viscoelastic properties of such LMOGs.

2.7. X-ray diffraction (XRD)

To get an idea of the aggregate sizes, XRD of the dried cast film of toluene gels was estimated. Interestingly, as the lipophilic segment of the alanine based gelator was increased, the diffraction angle (2θ) decreased (not shown) indicating a dramatic increase in the aggregate size. The parameters from XRD data are listed in Table 3. For shorter chains, we found more than one aggregate but with increasing chain length not only the sizes of aggregate increased but also only one aggregate morph predominated. For **2f** with a C18 chain the diffraction angle became even less than 2° indicating aggregate sizes were more than 44.7 Å.

2.8. Molecular modeling studies

Energy minimization of the structure of a simplified analog, ethanoyl-L-alanine 'tetramer' at restricted Hartree–Fock (RHF) level using 6-31G* basis sets shows that there is an existence of hydrogen bonding between the –COOH groups indicating strong acid dimer formation ($d_{O-H\cdots O}$=1.77–1.91 Å) (Fig. 6). The amide linkage also participates in hydrogen bonding ($d_{N-H\cdots O}$=2.20–2.51 Å) to connect two

Table 3. Parameters of XRD of xerogels and the long spacing of the aggregates

Gels in toluene	2θ (°)	d_{001} (Å)
2b	2.65, 2.92	33.3, 30.3
2c	2.35, 2.62	37.6, 33.7
2d	2.13, 2.28	41.5, 38.7
2e	2.13	41.5
2f	<2	44.2

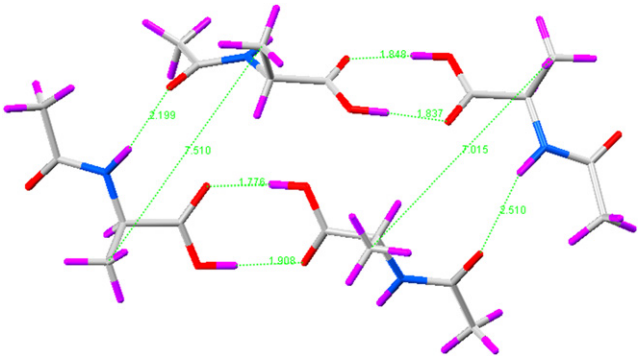

Figure 6. Energy minimized structure of the functional moiety of the gel formed by L-alanine based gelator molecule as indicated from restricted Hartree–Fock using 6-31G* level of theory (gray, purple, red, and blue colors represent carbon, hydrogen, oxygen, and nitrogen atoms, respectively).

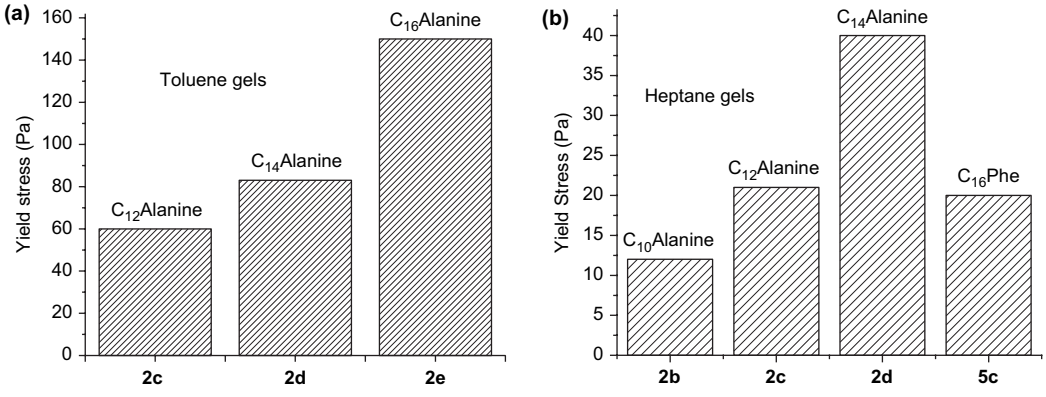

Figure 5. (a) Yield stresses of toluene gels of **2c**–**2e**. (b) Yield stresses of heptane gels of **2b**–**2d** and **5c**. Error in measurement is within ±5%.

acid dimers leading to a continuous assembly. Both of these facts have been experimentally verified from FTIR studies with the gelator dodecanoyl-L-alanine. So it is clear that the self-assembly of L-alanine derivatives ensues through these two types of hydrogen bonding and also that the side chain plays a role in packing the aggregate. The distance between the two carbons of the methyl groups remains within 7.01–7.51 Å. So an amino acid side chain larger than methyl poses steric constraints, which may impede efficient packing of the molecules leading to the formation of self-assembled organization. Thus in the case of most of the other amino acid based fatty acid amides, we observed either no gelation or the formation of a 'loose' or weak gel.

3. Conclusion

In this work, we have investigated the scope of gelation properties exhibited by various fatty acid amides of natural amino acids. It has been found that out of the six non-polar amino acids examined, L-alanine derivatives are best suited for the design of this class of gelators. The increase in the fatty acid chain length improves gel fiber mechanical strength and also the van der Waals contacts as well as the thermal stabilities. However, gelation number (capacity to retain solvent molecules) does not increase linearly with the fatty acid chain length. The viscoelastic flow behavior of the physical gels from this class of molecules is dependent on both the length of the fatty acid chain and the nature of the side chain of the amino acid.

Taking together the FTIR, XRD results, calculation of functional moiety of gelation at RHF level, and the gelation properties of various fatty acid amides of L-amino acids, it is plausible to conclude that the gel assemblies consist of layered structures. Within the layered framework, the fatty acid amides of L-amino acids are 'glued' together by intra- and interlayer hydrogen bondings leading to the formation of a hydrogen-bonded network. These networks develop into a supramolecular assembly. Gelation is a phenomenon exhibited by molecules that have the capacity to aggregate to form fibrous networks. Self-assembly of these systems into fibrous structures is evident from SEM. A particularly intriguing aspect of these molecules as gelators is that these are derived from naturally occurring sources, e.g., fatty acids and L-amino acid. These can be synthesized very easily and from inexpensive starting materials. So their use as gelators does not release any unnatural materials into the environment, making this class of LMOG excellent materials for various applications.

4. Experimental section

4.1. General

Melting points were recorded in open capillaries and are uncorrected. ^{1}H NMR spectra were recorded in Bruker-400 NMR spectrometer. Chemical shifts are reported in parts per million downfield from the internal standard, tetramethylsilane. FTIR studies were performed on a JASCO 410 model spectrometer and are reported in wavenumbers (cm^{-1}).

4.2. Materials

All reagents, starting materials, and silica gel for TLC and column chromatography were obtained from the best known commercial sources and were used without further purification, as appropriate. Glycine, L-alanine, L-valine, L-leucine, L-phenylalanine, L-tryptophan, *N*-methyl L-alanine and *N*-benzyloxycarbonyl alanine were purchased from Sigma. Compounds **20**, **22**, and **23** have been synthesized as reported previously.[19] Solvents were distilled and dried prior to use.

4.3. Synthesis

4.3.1. General procedure for the synthesis of *N*-acyl amino acid methyl ester derivatives. Individual amino acid methyl ester hydrochloride (**13–18**) (7.5 mmol) was dissolved in water (15 mL) and $KHCO_3$ (0.9 g, 9.0 mmol) was added to the solution at 0 °C. This solution was extracted with ether (5×10 mL) and dried over anhydrous Na_2SO_4. Ether was evaporated to give a transparent oil in yields >99%. Individual amino acid methyl ester (7.5 mmol) was dissolved in dry $CHCl_3$ (15 mL) to which triethylamine (0.76 g, 7.52 mmol) was added and cooled in ice. The desired acyl chloride (7.52 mmol) was added in the form of a solution in dry $CHCl_3$ (2 mL) dropwise to the ice-cold solution and stirred for 5 h. The reaction mixture was diluted with $CHCl_3$ (15 mL) and shaken with 3 M HCl (3×15 mL), water (15 mL), and brine (15 mL), and finally dried over anhydrous Na_2SO_4. The solvent was removed by rotary evaporation and the residue purified by column chromatography on silica gel using a mixture of ethyl acetate/hexanes. The relevant spectral and analytical data for each compound along with the isolated yields in parentheses are given below.

4.3.1.1. *N*-*n*-Dodecanoyl-methyl glycinate (7). Yield 1.91 g, 94%; mp=63–64 °C. IR (Neat): ν=3322, 2920, 2850, 1750, 1644, 1540 cm^{-1}. ^{1}H NMR (400 MHz, $CDCl_3$) δ 0.88 (t, 3H, J=7.0 Hz), 1.27 (br s, 16H), 1.61–1.70 (m, 2H), 2.24 (t, 2H, J=7.8 Hz), 3.77 (s, 3H), 4.05 (d, 2H, J=5.1 Hz), 5.98 (br s, 1H). ^{13}C NMR (100 MHz, $CDCl_3$) δ 14.09, 22.66, 25.55, 29.22, 29.31 (2C), 29.44, 29.57 (2C), 31.88, 36.41, 41.15, 52.34, 170.60, 173.31. HRMS (ESI^+) calcd for $(C_{15}H_{29}NO_3Na)^+$: 294.2045; found: 294.2041. Anal. Calcd for $C_{15}H_{29}NO_3$: C, 66.38; H, 10.77; N, 5.16. Found: C, 66.44; H, 10.54; N, 5.16.

4.3.1.2. *N*-*n*-Octanoyl methyl (L)-alaninate (8a). Yield 1.59 g, 93%. IR (Neat): ν=3295, 2929, 2857, 1749, 1650, 1544 cm^{-1}. ^{1}H NMR (400 MHz, $CDCl_3$) δ 0.88 (t, 3H, J=6.7 Hz), 1.23 (br s, 8H), 1.40 (d, 3H, J=7.2 Hz), 1.59–1.67 (m, 2H), 2.21 (t, 2H, J=7.8 Hz), 3.03 (s, 3H), 4.57–4.64 (m, 1H), 6.06 (d, 1H, J=4.8 Hz). ^{13}C NMR (100 MHz, $CDCl_3$) δ 14.02, 18.54, 22.55, 25.54, 28.95, 29.13, 31.63, 36.53, 47.82, 52.41, 172.67, 173.72. HRMS (ESI^+) calcd for $(C_{12}H_{23}NO_3Na)^+$: 252.1576; found: 252.1591.

4.3.1.3. *N*-*n*-Decanoyl methyl (L)-alaninate (8b). Yield 1.73 g, 90%. IR (Neat): ν=3294, 2926, 2855, 1750, 1650, 1545 cm^{-1}. ^{1}H NMR (300 MHz, $CDCl_3$) δ 0.85 (t, 3H, J=6.6 Hz), 1.24 (br s, 12H), 1.38 (d, 3H, J=7.2 Hz), 1.58–1.63 (m, 2H), 2.19 (t, 2H, J=7.8 Hz), 3.73 (s, 3H), 4.54–4.63 (m, 1H), 6.09 (br s, 1H). ^{13}C NMR (75 MHz, $CDCl_3$) δ 14.03, 18.49, 22.60, 25.53, 29.16, 29.20, 29.28, 29.38,

31.80, 36.48, 47.80, 52.37, 172.69, 173.69. HRMS (ESI^+) calcd for $(C_{14}H_{27}NO_3Na)^+$: 280.1889; found: 280.1869.

4.3.1.4. *N*-*n*-Dodecanoyl methyl (L)-alaninate (8c). Yield 2.07 g, 97%; mp=65 °C. IR (neat): ν=3300, 2920, 2851, 1732, 1650, 1537 cm^{-1}. ^1H NMR (400 MHz, $CDCl_3$) δ 0.88 (t, 3H, J=7.2 Hz), 1.28 (br s, 16H), 1.40 (d, 3H, J=7.1 Hz), 1.59–1.67 (m, 2H), 2.21 (t, 3H, J=7.8 Hz), 3.75 (s, 3H), 4.57–4.65 (m, 1H), 6.03 (d, 1H, J=6.8 Hz). ^{13}C NMR (100 MHz, $CDCl_3$) δ 14.07, 18.58, 22.65, 25.55, 29.20, 29.30 (2C), 29.44, 29.57 (2C), 31.88, 36.56, 47.84, 52.40, 172.64, 173.72. HRMS (ESI^+) calcd for $(C_{16}H_{31}NO_3Na)^+$: 308.2202; found: 308.2204. Anal. Calcd for $C_{16}H_{31}NO_3$: C, 67.33; H, 10.95; N, 4.91. Found: C, 67.52; H, 11.03; N, 5.05.

4.3.1.5. *N*-*n*-Tetradecanoyl methyl (L)-alaninate (8d). Yield 2.20 g, 94%; mp=69–71 °C. IR (neat): ν=3308, 2919, 2851, 1730, 1646, 1537 cm^{-1}. ^1H NMR (400 MHz, $CDCl_3$) δ 0.88 (t, 3H, J=7.0 Hz), 1.25 (br s, 20H), 1.40 (d, 3H, J=7.2 Hz), 1.61–1.66 (m, 2H), 2.20 (t, 3H, J=7.8 Hz), 3.75 (s, 3H), 4.57–4.65 (m, 1H), 5.98 (d, 1H, J=6.1 Hz). ^{13}C NMR (100 MHz, $CDCl_3$) δ 14.10, 18.62, 22.67, 25.57, 29.22, 29.33, 29.34, 29.47, 29.57 (2C), 29.63, 29.66, 31.91, 36.59, 47.87, 52.42, 172.63, 173.74. HRMS (ESI^+) calcd for $(C_{18}H_{35}NO_3Na)^+$: 336.2515; found: 336.2516. Anal. Calcd for $C_{18}H_{35}NO_3$: C, 68.97; H, 11.25; N, 4.47. Found: C, 69.02; H, 11.58; N, 4.60.

4.3.1.6. *N*-*n*-Hexadecanoyl methyl (L)-alaninate (8e). Yield 2.37 g, 93%; mp=77–78 °C. IR (Neat): ν=3395, 2918, 2851, 1732, 1646, 1539 cm^{-1}. ^1H NMR (400 MHz, $CDCl_3$) δ 0.88 (t, 3H, J=7.0 Hz), 1.25 (br s, 24H), 1.40 (d, 3H, J=7.2 Hz), 1.60–1.61 (m, 2H), 2.20 (t, 2H, J=7.9 Hz), 3.75 (s, 3H), 4.57–4.64 (m, 1H), 5.99 (br d, 1H, J=5.6 Hz). ^{13}C NMR (100 MHz, $CDCl_3$) δ 14.11, 18.62, 22.68, 25.56, 29.21, 29.33, 29.35, 29.47, 29.60, 29.64 (2C), 29.68 (3C), 31.91, 36.59, 47.85, 52.45, 172.64, 173.74. HRMS (ESI^+) calcd for $(C_{20}H_{39}NO_3Na)^+$: 364.2828; found: 364.2824. Anal. Calcd for $C_{20}H_{39}NO_3$: C, 70.33; H, 11.51; N, 4.10. Found: C, 70.36; H, 11.61; N, 4.16.

4.3.1.7. *N*-*n*-Octadecanoyl methyl (L)-alaninate (8f). Yield 2.69 g, 95%; mp=82–83 °C. IR (Neat): ν=3314, 2917, 2849, 1731, 1645, 1537 cm^{-1}. ^1H NMR (400 MHz, $CDCl_3$) δ 0.81 (t, 3H, J=7.0 Hz), 1.18 (br s, 28H), 1.39 (d, 3H, J=7.2 Hz), 1.52–1.58 (m, 2H), 2.13 (t, 2H, J=7.8 Hz), 3.71 (s, 3H), 4.49–4.59 (m, 1H), 5.97 (br d, 1H, J=6.6 Hz). ^{13}C NMR (75 MHz, $CDCl_3$) δ 14.10, 18.57, 22.67, 25.55, 29.20, 29.33 (2C), 29.44, 29.66 (8C), 31.89, 36.55, 47.82, 52.42, 172.67, 173.72. HRMS (ESI^+) calcd for $(C_{22}H_{43}NO_3Na)^+$ 392.3152; found: 392.3141. Anal. Calcd for $C_{22}H_{43}NO_3$: C, 71.50; H, 11.73; N, 3.79. Found: C, 71.60; H, 11.86; N, 4.05.

4.3.1.8. *N*-*n*-Dodecanoyl methyl (L)-valinate (9a). Yield 2.13 g, 91%; mp=41–43 °C. IR (Neat): ν=3306, 2926, 2855, 1746, 1650, 1540 cm^{-1}. ^1H NMR (400 MHz, $CDCl_3$) δ 0.88 (t, 3H, J=7.0 Hz), 0.92 (d, 3H, J=6.7 Hz), 0.95 (d, 3H, J=7.5 Hz), 1.25 (br s, 16H), 1.60–1.65 (m, 2H), 2.13–2.17 (m, 1H), 2.24 (t, 2H, J=7.4 Hz), 3.74 (s, 3H), 4.59 (dd, 1H, J_1=8.8 Hz, J_2=4.9 Hz), 5.96 (d, 1H, J=8.4 Hz). ^{13}C NMR (100 MHz, $CDCl_3$) δ 14.09, 17.72, 17.80, 18.90, 22.60, 24.75, 25.69, 29.22, 29.31, 29.46, 29.57, 31.31, 31.88, 36.73, 52.13, 56.79, 172.77, 173.20. HRMS (ESI^+) calcd for $(C_{18}H_{35}NO_3Na)^+$: 336.2512; found: 336.2515. Anal. Calcd for $C_{18}H_{35}NO_3$: C, 68.97; H, 11.25; N, 4.47. Found: C, 68.52; H, 11.33; N, 4.31.

4.3.1.9. *N*-*n*-Hexadecanoyl methyl (L)-valinate (9b). Yield 2.57 g, 93%; mp=68–69 °C. IR (Neat): ν=3292, 2915, 2848, 1736, 1647, 1538 cm^{-1}. ^1H NMR (400 MHz, $CDCl_3$) δ 0.81 (t, 3H, J=7.0 Hz), 0.83 (d, 3H, J=6.8 Hz), 0.87 (d, 3H, J=6.8 Hz), 1.23 (br s, 24H), 1.53–1.59 (m, 2H), 2.06–2.10 (m, 1H), 2.17 (t, 2H, J=7.5 Hz), 3.67 (s, 3H), 4.50–4.53 (m, 1H), 5.89 (d, 1H, J=8.4 Hz). ^{13}C NMR (100 MHz, $CDCl_3$) δ 14.12, 17.82, 18.93, 22.69, 25.71, 29.25, 29.34, 29.36, 29.49, 29.61 (2C), 29.65, 29.68 (3C), 31.32, 31.92, 36.75, 52.12, 56.78, 172.79, 173.10. HRMS (ESI^+) calcd for $(C_{22}H_{43}NO_3Na)^+$: 392.3141; found: 392.3118. Anal. Calcd for $C_{22}H_{43}NO_3$: C, 71.50; H, 11.73; N, 3.79. Found: C, 71.66; H, 12.02; N, 4.01.

4.3.1.10. *N*-*n*-Dodecanoyl methyl (L)-leucinate (10a). Yield 1.99 g, 81%. IR (Neat): ν=3287, 2925, 2855, 1751, 1650, 1546 cm^{-1}. ^1H NMR (400 MHz, $CDCl_3$) δ 0.88 (t, 3H, J=7.0 Hz), 0.93 (d, 3H, J=2.9 Hz), 0.95 (d, 3H, J=2.7 Hz), 1.25 (br s, 16H), 1.50–1.54 (m, 1H), 1.60–1.68 (m, 4H), 2.21 (t, 2H, J=7.8 Hz), 3.73 (s, 3H), 4.65 (dt, 1H, J_1=8.7 Hz, J_2=4.8 Hz), 5.84 (d, 1H, J=7.5 Hz). ^{13}C NMR (100 MHz, $CDCl_3$) δ 14.04, 21.95, 22.66, 22.78, 24.86, 25.57, 29.19, 29.30 (2C), 29.46, 29.57 (2C), 31.88, 36.57, 41.76, 50.48, 52.23, 172.91, 173.77. HRMS (ESI^+) calcd for $(C_{19}H_{37}NO_3Na)^+$: 350.2671; found: 350.2651. Anal. Calcd for $C_{19}H_{37}NO_3$: C, 69.68; H, 11.39; N, 4.28. Found: C, 69.84; H, 11.12; N, 4.46.

4.3.1.11. *N*-*n*-Hexadecanoyl methyl (L)-leucinate (10b). Yield 2.52 g, 88%; mp=52–53 °C. IR (Neat): ν=3327, 2915, 2848, 1754, 1644, 1528 cm^{-1}. ^1H NMR (400 MHz, $CDCl_3$) δ 0.87 (t, 3H, J=6.6 Hz), 0.93 (d, 3H, J=2.9 Hz), 0.94 (d, 3H, J=2.7 Hz), 1.28 (br s, 24H), 1.49–1.56 (m, 1H), 1.60–1.67 (m, 4H), 2.20 (t, 2H, J=7.4 Hz), 3.72 (s, 3H), 4.65 (dt, 1H, J_1=8.7 Hz, J_2=4.8 Hz), 5.84 (d, 1H, J=7.5 Hz). ^{13}C NMR (100 MHz, $CDCl_3$) δ 14.12, 21.97, 22.69, 22.80, 24.88, 25.59, 29.22, 29.34, 29.36, 29.50, 29.61 (4C), 29.65, 29.69, 31.93, 36.60, 41.78, 50.50, 52.26, 172.94, 173.80. HRMS (ESI^+) calcd for $(C_{23}H_{45}NO_3Na)^+$: 406.3297; found: 406.3271. Anal. Calcd for $C_{23}H_{45}NO_3$: C, 72.01; H, 11.82; N, 3.65. Found: C, 72.00; H, 11.64; N, 3.73.

4.3.1.12. *N*-*n*-Hexanoyl methyl (L)-phenylalaninate (11a). Yield 1.74 g, 72%. IR (Neat): ν=3292, 2955, 2860, 1747, 1650, 1542 cm^{-1}. ^1H NMR (400 MHz, $CDCl_3$) δ 0.88 (t, 3H, J=7.0 Hz), 1.22–1.32 (br m, 4H), 1.54–1.61 (m, 2H), 2.16 (t, 2H, J=7.8 Hz), 3.07 (dd, 1H, J_1=13.7 Hz, J_2=5.5 Hz), 3.15 (dd, 1H, J_1=13.8 Hz, J_2=5.8 Hz), 3.72 (s, 3H), 4.88–4.92 (m, 1H), 6.04 (br s, 1H), 7.09 (dd, 2H, J_1=6.7 Hz, J_2=1.2 Hz), 7.21–7.29 (m, 3H). ^{13}C NMR (100 MHz, $CDCl_3$) δ 13.79, 22.24, 25.12, 31.21, 36.33, 37.78, 52.17, 52.82, 127.97, 128.42 (2C), 129.13 (2C), 135.83, 172.14, 172.68. HRMS (ESI^+) calcd for $(C_{16}H_{23}NO_3Na)^+$: 300.1576; found: 300.1572.

4.3.1.13. *N*-*n*-Dodecanoyl methyl (L)-phenylalaninate (11b). Yield 2.25 g, 83%; mp=54–56 °C. IR (Neat):

ν=3300, 2911, 2850, 1740, 1650, 1530 cm^{-1}. ^1H NMR (300 MHz, $CDCl_3$) δ 0.88 (t, 3H, J=6.6 Hz), 1.25 (br s, 16H), 1.56–1.60 (m, 2H), 2.16 (t, 2H, J=7.8 Hz), 3.07–3.19 (m, 2H), 3.73 (s, 3H), 4.87–4.93 (m, 1H), 5.88 (d, 1H, J=6.6 Hz), 7.08 (dd, 2H, J_1=5.7 Hz, J_2=1.8 Hz), 7.24–7.31 (m, 3H). ^{13}C NMR (100 MHz, $CDCl_3$) δ 14.09, 22.66, 25.53, 29.17, 29.24, 29.30, 29.43, 29.58 (2C), 31.88, 36.55, 37.89, 52.29, 52.86, 127.08, 128.53 (2C), 129.23 (2C), 135.85, 172.28, 172.70. HRMS (ESI^+) calcd for $(C_{22}H_{35}NO_3Na)^+$: 384.2515; found: 384.2518. Anal. Calcd for $C_{22}H_{35}NO_3$: C, 73.09; H, 9.76; N, 3.87. Found: C, 72.83; H, 9.88; N, 3.95.

4.3.1.14. *N*-*n*-Hexadecanoyl methyl (L)-phenylalaninate (11c). Yield 2.32 g, 74%; mp=72–73 °C. IR (Neat): ν=3324, 2916, 2849, 1744, 1647, 1532 cm^{-1}. ^1H NMR (400 MHz, $CDCl_3$) δ 0.88 (t, 3H, J=7.0 Hz), 1.25 (br s, 24H), 1.56–1.59 (m, 2H), 2.16 (t, 2H, J=7.8 Hz), 3.09 (dd, 1H, J_1=13.8 Hz, J_2=5.7 Hz), 3.16 (dd, 1H, J_1=13.8 Hz, J_2=5.8 Hz), 3.73 (s, 3H), 4.91 (dt, 1H, J_1=7.8 Hz, J_2=5.8 Hz), 5.86 (d, 1H, J=7.6 Hz), 7.08 (dd, 2H, J_1=7.2 Hz, J_2=1.2 Hz), 7.24–7.31 (m, 3H). ^{13}C NMR (100 MHz, $CDCl_3$) δ 14.10, 22.67, 25.53, 29.19, 29.31, 29.34, 29.45, 29.59, 29.63, 29.66, 29.68 (2C), 31.91 (2C), 36.56, 37.90, 52.29, 52.86, 127.09, 128.53 (2C), 129.24 (2C), 135.86, 172.17, 172.67. HRMS (ESI^+) calcd for $(C_{26}H_{43}NO_3Na)^+$: 440.3141; found: 440.3141. Anal. Calcd for $C_{28}H_{47}NO_3$: C, 74.77; H, 10.38; N, 3.35. Found: C, 74.73; H, 10.48; N, 3.57.

4.3.1.15. *N*-*n*-Octadecanoyl methyl (L)-phenylalaninate (11d). Yield 2.53 g, 76%; mp=75–76 °C. IR (Neat): ν=3327, 2916, 2850, 1746, 1648, 1532 cm^{-1}. ^1H NMR (400 MHz, $CDCl_3$) δ 0.81 (t, 3H, J=7.0 Hz), 1.18 (br s, 28H), 1.49–1.52 (m, 2H), 2.09 (t, 2H, J=8.0 Hz), 3.02 (dd, 1H, J_1=13.8 Hz, J_2=5.8 Hz), 3.09 (dd, 1H, J_1=13.8 Hz, J_2=5.8 Hz), 3.66 (s, 3H), 4.84 (dt, 1H, J_1=5.8 Hz, J_2=2.0 Hz), 5.81 (d, 1H, J=7.8 Hz), 7.02 (dd, 2H, J_1=6.5 Hz, J_2=1.5 Hz), 7.17–7.23 (m, 3H). ^{13}C NMR (100 MHz, $CDCl_3$) δ 14.08, 22.66, 25.53, 29.18, 29.31, 29.34, 29.45, 29.60, 29.64, 29.68 (6C), 31.91, 36.56, 37.92, 52.27, 52.88, 127.09, 128.53 (2C), 129.24 (2C), 135.88, 172.18, 172.69. HRMS (ESI^+) calcd for $(C_{28}H_{47}NO_3Na)^+$: 468.3454; found: 468.3457. Anal. Calcd for $C_{28}H_{47}NO_3$: C, 75.46; H, 10.63; N, 3.14. Found: C, 75.69; H, 10.55; N, 3.30.

4.3.1.16. *N*-*n*-Dodecanoyl methyl (L)-tryptophanate (12a). Yield 2.49 g, 83%; mp=68–69 °C. IR (Neat): ν=3300, 2925, 2853, 1740, 1651, 1530 cm^{-1}. ^1H NMR (400 MHz, $CDCl_3$) δ 0.88 (t, 3H, J=7.2 Hz), 1.27 (br s, 16H), 1.54–1.58 (m, 2H), 2.13 (t, 2H, J=8.1 Hz), 3.32 (dd, 2H, J_1=5.2 Hz, J_2=2.4 Hz), 3.69 (s, 3H), 4.97 (dt, 1H, J_1=9.3 Hz, J_2=5.3 Hz), 5.96 (d, 1H, J=7.8 Hz), 6.97 (d, 1H, J=2.3 Hz), 7.11 (dt, 1H, J_1=8 Hz, J_2=1 Hz), 7.17 (dt, 1H, J_1=8 Hz, J_2=0.4 Hz), 7.36 (dd, 1H, J_1=8 Hz, J_2=0.4 Hz), 7.53 (dd, 1H, J_1=8 Hz, J_2=0.4 Hz), 8.12 (br s, 1H). ^{13}C NMR (100 MHz, $CDCl_3$) δ 14.10, 22.66, 25.45, 27.64, 29.21, 29.30, 29.32, 29.44, 29.58 (2C), 31.89, 36.61, 52.30, 52.83, 110.16, 111.23, 118.58, 119.67, 122.24, 122.61, 127.71, 136.06, 172.51, 172.79. HRMS (ESI^+) calcd for $(C_{24}H_{36}N_2O_3Na)^+$: 423.2624; found: 423.2610. Anal. Calcd for $C_{24}H_{36}N_2O_3$: C, 71.96; H, 9.06; N, 6.99. Found: C, 71.90; H, 9.18; N, 6.92.

4.3.1.17. *N*-*n*-Hexadecanoyl methyl (L)-tryptophanate (12b). Yield 2.73 g, 80%; mp=69–70 °C. IR (Neat): ν=3385, 2923, 2852, 1740, 1650, 1536 cm^{-1}. ^1H NMR (400 MHz, $CDCl_3$) δ 0.80 (t, 3H, J=7.0 Hz), 1.18 (br s, 24H), 1.46–1.50 (m, 2H), 2.08 (t, 2H, J=8.0 Hz), 3.23 (dd, 2H, J_1=6.0 Hz, J_2=2.5 Hz), 3.60 (s, 3H), 4.89 (dt, 1H, J_1=7.4 Hz, J_2=5.4 Hz), 5.95 (d, 1H, J=7.7 Hz), 6.87 (d, 1H, J=2.0 Hz), 7.02 (t, 1H, J=7.2 Hz), 7.10 (t, 1H, J=7.2 Hz), 7.26 (d, 1H, J=8.1 Hz), 7.44 (d, 1H, J=7.9 Hz), 8.38 (br s, 1H). ^{13}C NMR (100 MHz, $CDCl_3$) δ 14.07, 22.64, 25.43, 27.60, 29.17, 29.28, 29.31, 29.42, 29.57 (2C), 29.61 (3C), 29.65, 31.87, 36.54, 52.27, 52.87, 109.88, 111.29, 118.46, 119.55, 122.17, 122.71, 127.65, 136.09, 172.51, 172.93. HRMS (ESI^+) calcd for $(C_{28}H_{44}N_2O_3Na)^+$: 479.3250; found: 479.3248. Anal. Calcd for $C_{28}H_{44}N_2O_3 \cdot 0.75H_2O$: C, 71.53; H, 9.75; N, 5.96. Found: C, 71.41; H, 9.68; N, 5.89.

4.3.1.18. *N*-*n*-Octadecanoyl methyl (L)-tryptophanate (12c). Yield 2.97 g, 82% mp=71–73 °C. IR (Neat): ν=3393, 2917, 2849, 1731, 1645, 1542 cm^{-1}. ^1H NMR (400 MHz, $CDCl_3$) δ 0.81 (t, 3H, J=7.0 Hz), 1.18 (br s, 28H), 1.45–1.51 (m, 2H), 2.06 (t, 2H, J=7.8 Hz), 3.25 (dd, 2H, J_1=5.3 Hz, J_2=2.5 Hz), 3.62 (s, 3H), 4.90 (dt, 1H, J_1=8.0 Hz, J_2=5.3 Hz), 5.90 (d, 1H, J=7.8 Hz), 6.89 (d, 1H, J=2.2 Hz), 7.04 (dt, 1H, J_1=7.9 Hz, J_2=0.8 Hz), 7.11 (dt, 1H, J_1=7.1 Hz, J_2=1.0 Hz), 7.28 (d, 1H, J=8.1 Hz), 7.45 (d, 1H, J=7.9 Hz), 8.15 (br s, 1H). ^{13}C NMR (100 MHz, $CDCl_3$) δ 14.10, 22.67, 25.45, 27.63, 29.21, 29.30, 29.34, 29.45, 29.60 (6C), 29.64, 29.68, 31.90, 36.60, 52.30, 52.84, 110.12, 111.24, 118.56, 119.65, 122.22, 122.63, 127.70, 136.06, 172.52, 172.83. HRMS (ESI^+) calcd for $(C_{30}H_{48}N_2O_3Na)^+$: 507.3563; found: 507.3563. Anal. Calcd for $C_{30}H_{48}N_2O_3$: C, 74.34; H, 9.98; N, 5.78. Found: C, 74.07; H, 9.83; N, 5.67.

4.3.2. General procedure for the synthesis of *N*-alkanoyl amino acid derivatives. Individual *N*-alkanoyl amino acid methyl ester (1.2 mmol) was dissolved in 3 mL of a 1:1 mixture of MeOH and THF. A cold solution of NaOH (0.048 g, 1.2 mmol) in water (1.5 mL) was added to the solution of ester at 0 °C and stirred for 2 h. The solvent was removed in vacuo, the aqueous residue was cooled in ice, and 6 M HCl (5 mL) was added dropwise. The white precipitate so formed was extracted in ethyl acetate (3×15 mL). The residue was precipitated in cold conditions three times from ethyl acetate/hexane.

4.3.2.1. *N*-*n*-Dodecanoyl-glycine (1). Yield 0.30 g, 98%; mp=119–120 °C. IR (Neat): ν=3315, 2917, 2849, 1702, 1643, 1554 cm^{-1}. ^1H NMR (400 MHz, $CDCl_3$) δ 0.88 (t, 3H, J=7.0 Hz), 1.28 (br s, 16H), 1.62–1.66 (m, 2H), 2.26 (t, 2H, J=7.5 Hz), 4.09 (d, 2H, J=5.2 Hz), 5.99 (br s, 1H). ^{13}C NMR (100 MHz, $CDCl_3$+1–2 drops of DMSO-d_6) δ 13.93, 22.65, 25.41, 29.07, 29.11, 29.15, 29.27, 29.39 (2C), 31.69, 36.18, 41.12, 171.70, 173.32. HRMS (ESI^+) calcd for $(C_{14}H_{27}NO_3Na)^+$: 280.1889; found: 280.1891. Anal. Calcd for $C_{14}H_{27}NO_3$: C, 65.33; H, 10.57; N, 5.44. Found: C, 65.51; H, 10.66; N, 5.30.

4.3.2.2. *N*-*n*-Octacanoyl (L)-alanine (2a). Yield 0.24 g, 98%. IR (Neat): ν=3395, 2918, 2851, 1707, 1646, 1539 cm^{-1}. ^1H NMR (400 MHz, $CDCl_3$) δ 0.87 (t, 3H, J=6.9 Hz), 1.28 (br s, 8H), 1.44 (d, 3H, J=7.2 Hz),

1.58–1.65 (m, 2H), 2.24 (t, 2H, J=7.2 Hz), 4.53–4.60 (m, 1H), 6.53 (br s, 1H). ^{13}C NMR (100 MHz, $CDCl_3$) δ 13.99, 18.06, 22.53, 25.56, 28.90, 29.06, 31.59, 36.35, 48.23, 174.19, 175.84. HRMS (ESI^+) calcd for $(C_{11}H_{21}NO_3Na)^+$: 238.1419; found: 238.1437.

4.3.2.3. *N*-*n*-Decanoyl (L)-alanine (2b). Yield 0.23 g, 93%; mp=63–64 °C. IR (Neat): ν=3346, 2920, 2851, 1706, 1646, 1526 cm^{-1}. ^{1}H NMR (400 MHz, $CDCl_3$) δ 0.88 (t, 3H, J=7.0 Hz), 1.26 (br s, 12H), 1.46 (d, 3H, J=7.2 Hz), 1.59–1.67 (m, 2H), 2.24 (t, 2H, J=7.6 Hz), 4.54–4.61 (m, 1H), 6.09 (br d, 1H, J=6.5 Hz). ^{13}C NMR (100 MHz, $CDCl_3$) δ 14.09, 17.89, 22.65, 25.51, 29.15, 29.24, 29.28, 29.40, 31.84, 36.42, 48.28, 174.07, 175.46. HRMS (ESI^+) calcd for $(C_{13}H_{25}NO_3Na)^+$: 226.1732; found: 226.1728. Anal. Calcd for $C_{13}H_{25}NO_3$: C, 64.16; H, 10.36; N, 5.76. Found: C, 64.43; H, 10.39; N, 5.96.

4.3.2.4. *N*-*n*-Dodecanoyl (L)-alanine (2c). Yield 0.31 g, 97%; mp=84 °C. IR (Neat): ν=3307, 2921, 2850, 1704, 1646, 1520 cm^{-1}. ^{1}H NMR (400 MHz, $CDCl_3$) δ 0.88 (t, 3H, J=7.0 Hz), 1.25 (br s, 16H), 1.46 (d, 3H, J=7.2 Hz), 1.59–1.64 (m, 2H), 2.24 (t, 2H, J=7.8 Hz), 4.54–4.61 (m, 1H), 6.09 (br s, 1H). ^{13}C NMR (100 MHz, $CDCl_3$) δ 14.06, 17.91, 22.67, 25.51, 29.16, 29.28, 29.31, 29.44, 31.89, 36.42, 48.28, 174.06, 175.52. HRMS (ESI^+) calcd for $(C_{15}H_{29}NO_3Na)^+$: 294.2045; found: 294.2025. Anal. Calcd for $C_{15}H_{29}NO_3$: C, 66.38; H, 10.77; N, 5.16. Found: C, 66.37; H, 10.67; N, 5.19.

4.3.2.5. *N*-*n*-Tetradecanoyl (L)-alanine (2d). Yield 0.34 g, 95%; mp=90–92 °C. IR (Neat): ν=3348, 2917, 2849, 1705, 1647, 1526 cm^{-1}. ^{1}H NMR (400 MHz, $CDCl_3$) δ 0.88 (t, 3H, J=7.0 Hz), 1.25 (br s, 20H), 1.46 (d, 3H, J=7.1 Hz), 1.58–1.64 (m, 2H), 2.24 (t, 2H, J=7.7 Hz), 4.53–4.58 (m, 1H), 6.20 (br d, 1H, J=6.5 Hz). ^{13}C NMR (100 MHz, $CDCl_3$) δ 14.11, 17.97, 22.68, 25.54, 29.17, 29.29, 29.34, 29.46, 29.60, 29.63 (2C), 29.67, 31.91, 36.43, 48.30, 174.08, 176.23. HRMS (ESI^+) calcd for $(C_{17}H_{33}NO_3Na)^+$: 322.2358; found: 322.2350. Anal. Calcd for $C_{17}H_{33}NO_3$: C, 68.19; H, 11.11; N, 4.68. Found: C, 68.43; H, 11.16; N, 4.45.

4.3.2.6. *N*-*n*-Hexadecanoyl (L)-alanine (2e). Yield 0.31 g, 94%; mp=91–93 °C. IR (Neat): ν=3315, 2917, 2849, 1704, 1646, 1528 cm^{-1}. ^{1}H NMR (400 MHz, $CDCl_3$) δ 0.88 (t, 3H, J=7.0 Hz), 1.25 (br s, 24H), 1.43 (d, 3H, J=7.1 Hz), 1.59–1.63 (m, 2H), 2.22 (t, 2H, J=7.6 Hz), 4.49–4.61 (m, 1H), 6.43 (br d, 1H, J=7.2 Hz). ^{13}C NMR (100 MHz, $CDCl_3$) δ 14.09, 17.98, 22.67, 25.59, 29.18, 29.23, 29.34, 29.45, 29.50, 29.59, 29.63, 29.64, 29.66, 29.69, 31.91, 36.41, 48.44, 174.07, 175.36. HRMS (ESI^+) calcd for $(C_{19}H_{37}NO_3Na)^+$: 350.2671; found: 350.2670. Anal. Calcd for $C_{19}H_{37}NO_3$: C, 69.68; H, 11.39; N, 4.28. Found: C, 69.66; H, 11.49; N, 4.15.

4.3.2.7. *N*-*n*-Octadecanoyl (L)-alanine (2f). Yield 0.39 g, 92%; mp=102–103 °C. IR (Neat): ν=3307, 2916, 2848, 1703, 1644, 1535 cm^{-1}. ^{1}H NMR (300 MHz, $CDCl_3$+1 drop of DMSO-d_6) δ 0.78 (t, 3H, J=7.2 Hz), 1.16 (br s, 28H), 1.32 (d, 3H, J=6.0 Hz), 1.50–1.55 (m, 2H), 2.11 (t, 2H, J=7.8 Hz), 4.42–4.62 (m, 1H), 6.32 (br d, 1H, J=7.2 Hz). ^{13}C NMR (75 MHz, $CDCl_3$+1 drop of DMSO-d_6) δ 13.96, 18.32, 22.50, 25.46, 29.07, 29.16 (2C), 29.31, 29.49 (8C), 31.73, 36.37, 47.80, 172.84, 174.84. HRMS (ESI^+) calcd for $(C_{21}H_{41}NO_3Na)^+$: 378.2977; found: 378.2984. Anal. Calcd for $C_{21}H_{41}NO_3$: C, 70.94; H, 11.62; N, 3.94. Found: C, 70.91; H, 11.59; N, 4.08.

4.3.2.8. *N*-*n*-Dodecanoyl (L)-valine (3a). Yield 0.32 g, 90%; mp=97–99 °C. IR (Neat): ν=3332, 2923, 2854, 1702, 1619, 1551 cm^{-1}. ^{1}H NMR (400 MHz, $CDCl_3$) δ 0.88 (t, 3H, J=7.0 Hz), 0.95 (d, 3H, J=6.9 Hz), 0.98 (d, 3H, J=6.8 Hz), 1.25 (br s, 16H), 1.60–1.65 (m, 2H), 2.21–2.35 (m, 3H), 4.57 (dd, 1H, J_1=8.6 Hz, J_2=4.8 Hz), 6.09 (d, 1H, J=8.6 Hz). ^{13}C NMR (100 MHz, $CDCl_3$) δ 14.09, 17.68, 18.99, 22.66, 25.70, 29.21, 29.29, 29.31, 29.46, 29.58 (2C), 30.91, 31.88, 36.67, 57.04, 174.04, 175.32. HRMS (ESI^+) calcd for $(C_{17}H_{33}NO_3Na)^+$: 322.2358; found: 322.2355. Anal. Calcd for $C_{17}H_{33}NO_3$: C, 68.19; H, 11.11; N, 4.68. Found: C, 67.68; H, 10.91; N, 4.17.

4.3.2.9. *N*-*n*-Hexadecanoyl (L)-valine (3b). Yield 0.39 g, 93%; mp=81–82 °C. IR (Neat): ν=3324, 2957, 2918, 2950, 1698, 1650, 1549 cm^{-1}. ^{1}H NMR (400 MHz, $CDCl_3$) δ 0.87 (t, 3H, J=7.0 Hz), 0.95 (d, 3H, J=7.2 Hz), 0.98 (d, 3H, J=6.8 Hz), 1.25 (br s, 24H), 1.60–1.65 (m, 2H), 2.21–2.27 (m, 3H), 4.56–4.59 (m, 1H), 6.10 (d, 1H, J=8.6 Hz). ^{13}C NMR (100 MHz, $CDCl_3$) δ 14.07, 17.69, 18.97, 22.66, 25.69, 29.31 (4C), 29.64 (6C), 30.92, 31.90, 36.67, 57.06, 174.05, 175.24. HRMS (ESI^+) calcd for $(C_{21}H_{41}NO_3Na)^+$: 378.2984; found: 378.2974. Anal. Calcd for $C_{21}H_{41}NO_3$: C, 70.94; H, 11.62; N, 3.94. Found: C, 70.91; H, 11.39; N, 3.93.

4.3.2.10. *N*-*n*-Dodecanoyl (L)-leucine (4a). Yield 0.37 g, 98%; mp=106–107 °C. IR (Neat): ν=3329, 2923, 2853, 1698, 1621, 1553 cm^{-1}. ^{1}H NMR (400 MHz, $CDCl_3$) δ 0.88 (t, 3H, J=7.0 Hz), 0.95 (d, 3H, J=2.9 Hz), 0.96 (d, 3H, J=3.2 Hz), 1.25 (br s, 16H), 1.53–1.64 (m, 3H), 1.66–1.76 (m, 2H), 2.24 (t, 2H, J=8.0 Hz), 4.62 (dt, 1H, J_1=8.8 Hz, J_2=4.9 Hz), 6.01 (d, 1H, J=7.5 Hz). ^{13}C NMR (100 MHz, $CDCl_3$) δ 14.09, 21.85, 22.66, 22.81, 24.87, 25.58, 29.18, 29.29, 29.32, 29.47, 29.59 (2C), 31.89, 36.49, 41.12, 50.84, 174.10, 176.31. HRMS (ESI^+) calcd for $(C_{18}H_{35}NO_3Na)^+$: 336.2515; found: 336.2500. Anal. Calcd for $C_{18}H_{35}NO_3$: C, 68.97; H, 11.25; N, 4.47. Found: C, 69.19; H, 11.25; N, 4.52.

4.3.2.11. *N*-*n*-Hexadecanoyl (L)-leucine (4b). Yield 0.40 g, 91%; mp=90–92 °C. IR (Neat): ν=3322, 2916, 2849, 1699, 1645, 1535 cm^{-1}. ^{1}H NMR (400 MHz, $CDCl_3$) δ 0.87 (t, 3H, J=6.8 Hz), 0.91 (d, 3H, J=3.4 Hz), 0.94 (d, 3H, J=4.4 Hz), 1.24 (br s, 24H), 1.55–1.65 (m, 3H), 1.68–1.71 (m, 2H), 2.24 (t, 2H, J=8.0 Hz), 4.55 (dt, 1H, J_1=8.0 Hz, J_2=4.0 Hz), 6.21 (d, 1H, J=7.6 Hz). ^{13}C NMR (100 MHz, $CDCl_3$) δ 14.06, 21.82, 22.65, 22.85, 24.91, 25.62, 29.33 (6C), 29.66 (4C), 31.90, 36.48, 41.18, 51.06, 174.18, 176.49. HRMS (ESI^+) calcd for $(C_{22}H_{43}NO_3Na)^+$: 392.3141; found: 392.3145. Anal. Calcd for $C_{22}H_{43}NO_3$: C, 71.50; H, 11.73; N, 3.79. Found: C, 71.35; H, 12.01; N, 3.94.

4.3.2.12. *N*-*n*-Hexanoyl (L)-phenylalanine (5a). Yield 0.25 mg, 78%; mp=137–139 °C. IR (cm^{-1}): 3303, 2928, 2868, 1708, 1611, 1555 cm^{-1}. ^{1}H NMR (400 MHz, $CDCl_3$) δ 0.87 (t, 3H, J=7.0 Hz), 1.18–1.26 (br m, 4H),

1.45–1.53 (m, 2H), 2.12 (t, 2H, J=7.8 Hz), 3.06 (dd, 1H, J_1=14.0 Hz, J_2=6.0 Hz), 3.17 (dd, 1H, J_1=14.0 Hz, J_2=5.6 Hz), 4.79–4.84 (m, 1H), 5.98 (d, 1H, J=7.6 Hz), 7.09 (dd, 2H, J_1=6.4 Hz, J_2=2.0 Hz), 7.16–7.24 (m, 3H). ^{13}C NMR (100 MHz, $CDCl_3$) δ 13.84, 22.28, 25.19, 31.22, 36.38, 37.27, 53.12, 127.20, 125.62 (2C), 129.34 (2C), 135.71, 174.03, 174.51. HRMS (ESI^+) calcd for $(C_{15}H_{21}NO_3Na)^+$: 286.1419; found: 286.1418. Anal. Calcd for $C_{15}H_{21}NO_3$: C, 68.42; H, 8.04; N, 5.32. Found: C, 68.33; H, 8.01; N, 5.64.

4.3.2.13. *N*-*n*-Dodecanoyl (L)-phenylalanine (5b). Yield 0.37 g, 98%; mp=97–98 °C. IR (Neat): ν=3313, 2923, 2852, 1708, 1643, 1538 cm^{-1}. ^{1}H NMR (300 MHz, $CDCl_3$) δ 0.88 (t, 3H, J=6.6 Hz), 1.25 (br s, 16H), 1.54–1.57 (m, 2H), 2.18 (t, 2H, J=8.1 Hz), 3.12 (dd, 1H, J_1=14.4 Hz, J_2=5.7 Hz), 3.24 (dd, 2H, J_1=14.1 Hz, J_2=5.7 Hz), 4.85–4.91 (m, 1H), 6.01 (d, 1H, J=6.6 Hz), 7.14 (dd, 2H, J_1=6.2 Hz, J_2=2.9 Hz), 7.23–7.32 (m, 3H). ^{13}C NMR (100 MHz, $CDCl_3$) δ 14.09, 22.66, 25.51, 29.12, 29.27, 29.32, 29.43, 29.59 (3C), 31.89, 36.44, 37.21, 53.09, 127.21, 128.62 (2C), 129.32 (2C), 135.65, 173.96, 174.56. HRMS (ESI^+) calcd for $(C_{21}H_{33}NO_3Na)^+$: 370.2358; found: 370.2357. Anal. Calcd for $C_{21}H_{33}NO_3$: C, 72.58; H, 9.59; N, 4.03. Found: C, 72.61; H, 9.96; N, 4.25.

4.3.2.14. *N*-*n*-Hexadecanoyl (L)-phenylalanine (5c). Yield 0.43 g, 95%; mp=83–86 °C. IR (Neat): ν=3302, 2920, 2851, 1709, 1644, 1536 cm^{-1}. ^{1}H NMR (400 MHz, $CDCl_3$) δ 0.88 (t, 3H, J=7.0 Hz), 1.25 (br s, 24H), 1.54–1.57 (m, 2H), 2.18 (t, 2H, J=7.9 Hz), 3.12 (dd, 1H, J_1=13.8 Hz, J_2=6.3 Hz), 3.24 (dd, 2H, J_1=14.1 Hz, J_2=5.6 Hz), 4.85–4.90 (m, 1H), 5.94 (d, 1H, J=6.1 Hz), 7.16 (dd, 2H, J_1=6.9 Hz, J_2=1.5 Hz), 7.26–7.32 (m, 3H). ^{13}C NMR (100 MHz, $CDCl_3$) δ 14.11, 22.68, 25.51, 29.13, 29.29, 29.35, 29.45, 29.61, 29.65 (2C), 29.69 (3C), 31.91, 36.45, 37.19, 53.13, 127.24, 128.66 (2C), 129.31 (2C), 135.65, 173.96, 174.35. HRMS (ESI^+) calcd for $(C_{25}H_{41}NO_3Na)^+$: 426.2984; found: 426.2962. Anal. Calcd for $C_{25}H_{41}NO_3$: C, 74.40; H, 10.74; N, 3.47. Found: C, 74.29; H, 10.50; N, 3.57.

4.3.2.15. *N*-*n*-Octadecanoyl (L)-phenylalanine (5d). Yield 0.48 g, 93%; mp=84–86 °C. IR (Neat): ν=3315, 2917, 2850, 1714, 1650, 1539 cm^{-1}. ^{1}H NMR (300 MHz, $CDCl_3$) δ 0.84 (t, 3H, J=7.0 Hz), 1.21 (br s, 28H), 1.49–1.55 (m, 2H), 2.15 (t, 2H, J=7.6 Hz), 3.10 (dd, 1H, J_1=13.6 Hz, J_2=6.1 Hz), 3.21 (dd, 2H, J_1=14.0 Hz, J_2=5.8 Hz), 4.81–4.87 (m, 1H), 6.01 (d, 1H, J=6.3 Hz), 7.13 (d, 2H, J=6.9 Hz), 7.20–7.28 (m, 3H). ^{13}C NMR (75 MHz, $CDCl_3$) δ 14.11, 22.68, 25.51, 29.13, 29.29, 29.35, 29.46, 29.69 (9C), 31.91, 36.43, 37.21, 53.14, 127.19, 128.62 (2C), 129.31 (2C), 135.71, 173.68, 174.36. HRMS (ESI^+) calcd for $(C_{27}H_{45}NO_3Na)^+$: 454.3297; found: 454.3297. Anal. Calcd for $C_{25}H_{41}NO_3$: C, 75.13; H, 10.51; N, 3.24. Found: C, 75.12; H, 10.84; N, 3.48.

4.3.2.16. *N*-*n*-Dodecanoyl (L)-tryptophan (6a). Yield 0.45 g, 98%; mp=107–109 °C. IR (Neat): ν=3409, 2925, 2854, 1722, 1648, 1525 cm^{-1}. ^{1}H NMR (300 MHz, $CDCl_3$) δ 0.88 (t, 3H, J=6.9 Hz), 1.25 (br m, 16H), 1.48–1.53 (m, 2H), 2.11 (t, 2H, J=7.2 Hz), 3.31–3.40 (m, 2H), 4.84–4.96 (m, 1H), 6.05 (d, 1H, J=7.6 Hz), 7.01 (d, 1H, J=8.1 Hz), 7.14 (t, 1H, J=7.2 Hz), 7.17 (t, 1H, J=7.2 Hz), 7.35 (d, 1H, J=8.4 Hz), 7.56 (d, 1H, J=8.0 Hz), 8.28 (s, 1H). ^{13}C NMR (100 MHz, $CDCl_3$) δ 14.11, 22.67, 25.37, 26.98, 29.13, 29.27, 29.33, 29.42, 29.60 (2C), 31.90, 36.44, 53.27, 109.64, 111.37, 118.42, 119.79, 122.29, 123.11, 127.71, 136.08, 174.20, 174.74. HRMS (ESI^+) calcd for $(C_{23}H_{34}N_2O_3Na)^+$: 409.2467; found: 409.2462. Anal. Calcd for $C_{23}H_{34}N_2O_3$: C, 71.47; H, 8.87; N, 7.25. Found: C, 71.45; H, 9.12; N, 7.06.

4.3.2.17. *N*-*n*-Hexadecanoyl (L)-tryptophan (6b). Yield 0.48 g, 91%; mp=95–97 °C. IR (Neat): ν=3414, 2923, 2852, 1720, 1632, 1536 cm^{-1}. ^{1}H NMR (400 MHz, $CDCl_3$) δ 0.81 (t, 3H, J=6.4 Hz), 1.19 (br s, 24H), 1.40–1.44 (m, 2H), 2.01 (t, 2H, J=7.6 Hz), 3.21–3.23 (m, 2H), 4.84–4.88 (m, 1H), 6.06 (d, 1H, J=7.6 Hz), 6.90 (d, 1H, J=1.6 Hz), 7.03 (t, 1H, J=7.2 Hz), 7.11 (t, 1H, J=7.2 Hz), 7.26 (d, 1H, J=8.0 Hz), 7.49 (d, 1H, J=7.6 Hz), 8.29 (br s, 1H). ^{13}C NMR (100 MHz, $CDCl_3$) δ 14.08, 22.67, 25.38, 27.08, 29.16, 29.33, 29.45 (2C), 29.67 (6C), 31.91, 36.42, 53.34, 109.58, 111.39, 118.39, 119.72, 122.20, 123.19, 127.78, 136.14, 174.28, 175.05. HRMS (ESI^+) calcd for $(C_{27}H_{42}N_2O_3Na)^+$: 465.3093; found: 465.3114. Anal. Calcd for $C_{27}H_{42}N_2O_3$: C, 73.26; H, 9.56; N, 6.33. Found: C, 73.19; H, 9.59; N, 6.14.

4.3.2.18. *N*-*n*-Octadecanoyl (L)-tryptophan (6c). Yield 0.49 g, 88%; mp=95–97 °C. IR (Neat): ν=3415, 2920, 2851, 1722, 1646, 1525 cm^{-1}. ^{1}H NMR (400 MHz, $CDCl_3$) δ 0.81 (t, 3H, J=6.4 Hz), 1.18 (br s, 28H), 1.36–1.43 (m, 2H), 1.99 (t, 2H, J=7.6 Hz), 3.21–3.30 (m, 2H), 4.82–4.87 (m, 1H), 6.08 (br s, 1H), 6.89 (s, 1H), 7.02 (t, 1H, J=6.4 Hz), 7.10 (t, 1H, J=6.4 Hz), 7.24 (dd, 1H, J_1=8.1 Hz, J_2=2.8 Hz), 7.47 (d, 1H, J=7.9 Hz), 8.32 (br d, 1H, J=8.1 Hz). ^{13}C NMR (100 MHz, $CDCl_3$) δ 14.11, 22.68, 25.39, 27.04, 29.15, 29.29, 29.35, 29.47, 29.65 (2C), 29.68, 29.71 (5C), 31.91, 36.40, 53.34, 109.49, 111.40, 118.36, 119.68, 122.16, 123.20, 127.75, 136.07, 174.31, 175.08. HRMS (ESI^+) calcd for $(C_{29}H_{46}N_2O_3Na)^+$: 493.3406; found: 493.3399.

4.4. Gelation studies

In a typical gelation number determination experiment, to a weighed amount of a particular compound in a test tube was added an excess of the chosen solvent. The resulting mixture was warmed till the compound dissolved. The solution was then allowed to cool to room temperature. Upon waiting for some time, a part of the solvent started to develop into a viscoelastic mass. This was allowed to settle and upon inversion of the test tube the excess ungelated solvent could be decanted out leaving the gelated mass inside the tube. On subtraction of the decanted solvent from the initially added solvent one could estimate the amount of solvent entrapped in the assembly. If a gel was formed it was evaluated quantitatively by determining the gelation number, which is the mole ratio of entrapped solvent and gelator dictating the number of solvent molecule that get immobilized per molecule of gelator. Each experiment was performed in duplicate.

4.5. Scanning electron microscopy

The gels were carefully scooped onto the brass stubs and were allowed to dry overnight in air. The samples were

further dried in a vacuum for 1 h, then coated with gold vapor, and analyzed on a Quanta 200 SEM operated at 5 KV.

4.6. Differential scanning calorimetry

Gel samples in different solvents were prepared as mentioned above and their thermotropic behavior was investigated using a high sensitivity differential scanning calorimetry using a CSC-4100 model multi-cell differential scanning calorimeter (Calorimetric Sciences Corporation, Utah, USA).

Gels were heated to sol and 0.4 mL clear sols were taken into DSC ampoules. The ampoules were sealed and the gels were allowed to set overnight at ambient conditions. The calorimetric measurement was carried out in the temperature range of 10–80 °C at a scan rate of 20 °C/h. At least two to three consecutive heating and cooling scans were performed. Baseline thermograms were obtained using same amount of the solvent in the respective DSC cells. The thermograms for the gel were obtained by subtracting the respective baseline thermogram from the sample thermogram using 'CpCalc' software provided by the manufacturer.

4.7. Rheological studies

An Anton Paar 100 rheometer using cone and plate geometries (CP 25-2) was utilized. The gap distance between the cone and the plate was fixed at 0.05 mm. The gel was scooped on the plate of the rheometer. Stress amplitude sweep experiment was performed at a constant oscillation frequency of 1 Hz for the strain range 0.001–100 at 20 °C. The rheometer has a built-in computer, which converts the torque measurements into either G' (the storage modulus) or G'' (the loss modulus) in oscillatory shear experiments.

4.8. X-ray diffraction studies

Various samples of gels (10 mg/mL) were individually placed carefully on a pre-cleaned glass slide and left to air dry for 8 h in a dust free environment. This yielded the self-supported cast films of xerogel on which measurements were performed using a Phillips X-ray diffractometer. The X-ray beam generated with a Cu anode at the wavelength of Kα beam at 1.5418 Å was directed toward the film edge and scanning was done up to a 2θ value of 12°. Data were analyzed and interpreted using the Bragg equation.

4.9. Molecular modeling studies

To minimize computation time, ethanoyl-L-alanine, a simplified analog of best gelator, *n*-dodecanoyl-L-alanine, was drawn on a Gaussview software. With the coordinates obtained from the software, the molecule was energy minimized using restricted Hartree–Fock (RHF 6-31-G*) level of computations. Then with the coordinates of the energy minimized model of the monomeric unit, an initial 'dimeric' model, involving the carboxylic acid H-bonding, was constructed using the Chem 3D software, which was optimized at RHF/6-31G* level of theory. Thereafter, a 'tetrameric' unit of the self-assembly was modeled from the optimized geometry of the molecular dimer and energy minimized using restricted Hartree–Fock at the same level.

Acknowledgements

We are grateful to the Department of Biotechnology, New Delhi, for financial support. We thank the Institute Nanoscience Initiative and the Department of Science and Technology, Government of India for SEM and Mr. Saikat Sen for help with molecular modeling.

References and notes

1. George, M.; Weiss, R. G. *Acc. Chem. Res.* **2006**, *39*, 489–497.
2. (a) Abdallah, D. J.; Weiss, R. G. *Adv. Mater.* **2000**, *12*, 1237–1247; (b) Bhattacharya, S.; Maitra, U.; Mukhopadhya, S.; Srivastava, A. *Molecular Gel: Materials with Self-Assembled Fibrillar Networks*; Weiss, R. G., Terech, P., Eds.; Springer: Netherlands, 2005; pp 613–647.
3. (a) Langer, R. *Acc. Chem. Res.* **2000**, *33*, 94–101; (b) Yang, Z.; Liang, G.; Xu, B. *Chem. Commun.* **2006**, 738–740.
4. Abdallah, D. J.; Weiss, R. G. *Langmuir* **2000**, *16*, 352–355.
5. (a) Bhattacharya, S.; Acharya, S. N. G.; Raju, A. R. *Chem. Commun.* **1996**, 2101–2102; (b) Suzuki, M.; Sato, T.; Kurose, A.; Shirai, H.; Hanabusa, K. *Tetrahedron Lett.* **2005**, *46*, 2741–2745; (c) Suzuki, M.; Sato, T.; Shirai, H.; Hanabusa, K. *Chem. Commun.* **2006**, 377–379.
6. (a) Hafkamp, R. J. H.; Feiters, M. C.; Nolte, R. J. M. *J. Org. Chem.* **1999**, *64*, 412–426; (b) Srivastava, A.; Ghorai, S.; Bhattacharjya, A.; Bhattacharya, S. *J. Org. Chem.* **2005**, *70*, 6574–6582; (c) Bhattacharya, S.; Acharya, S. N. G. *Chem. Mater.* **1999**, *11*, 3121–3132.
7. Jang, W. D.; Jiang, D. L.; Aida, T. *J. Am. Chem. Soc.* **2000**, *122*, 3232–3233.
8. (a) Geiger, C.; Stanesau, M.; Chen, L.; Whitten, D. G. *Langmuir* **1999**, *15*, 2241–2245; (b) Terech, P.; Ostani, E.; Weiss, R. G. *J. Phys. Chem.* **1996**, *100*, 3759–3766; (c) Sangeetha, N. M.; Maitra, U. *Chem. Soc. Rev.* **2005**, *34*, 821–836.
9. Kuroiwa, K.; Shibata, T.; Takada, A.; Nemoto, N.; Kimizuka, N. *J. Am. Chem. Soc.* **2004**, *126*, 2016–2021.
10. (a) Inoue, K.; Ono, Y.; Kanakiyo, Y.; Ishi, I. T.; Yoshihara, K.; Shinkai, S. *J. Org. Chem.* **1999**, *64*, 2933–2937; (b) Maitra, U.; Kumar, P. V.; Chandra, N.; D'Souza, L. J.; Prasanna, M. D.; Raju, A. R. *Chem. Commun.* **1999**, 595–596; (c) Hirst, A. R.; Smith, D. K. *Chem.—Eur. J.* **2005**, *11*, 5496–5508.
11. (a) Oda, R.; Huc, I.; Candau, S. J. *Angew. Chem., Int. Ed.* **1998**, *37*, 2689–2691; (b) Bhattacharya, S.; De, S. *Langmuir* **1999**, *15*, 3400–3410; (c) Kimura, T.; Shinkai, S. *Chem. Lett.* **1998**, 1035–1036; (d) Gradzielski, M.; Bergmeier, M.; Muller, M.; Hoffman, H. *J. Phys. Chem. B* **1997**, *101*, 1719–1722.
12. Luo, X.; Liu, B.; Liang, Y. *Chem. Commun.* **2001**, 1556–1557.
13. Bhattacharya, S.; Krisnan-Ghosh, Y. *Chem. Commun.* **2001**, 185–186; See also: *Chem. Eng. News* **2001**, *Jan 29*, 12.
14. (a) Trivedi, D. R.; Ballabh, A.; Dastidar, P.; Ganguly, B. *Chem.—Eur. J.* **2004**, *10*, 5311–5322; (b) Couffin-Hoarau, A.; Motulsky, A.; Delmas, P.; Leroux, J. *Pharm. Res.* **2004**, *21*, 454–457.
15. Motulsky, A.; Lafleur, M.; Couffin-Hoarau, A.-C.; Hoarau, D.; Boury, F.; Benoit, J.-P.; Leroux, J.-C. *Biomaterials* **2005**, *26*, 6242–6253.
16. Bhattacharya, S.; Srivastava, A.; Pal, A. *Angew. Chem., Int. Ed.* **2006**, *45*, 2934–2937.
17. Ray, S.; Das, A. K.; Banerjee, A. *Chem. Commun.* **2006**, 2816–2818.

18. (a) Becerril, J.; Escuder, B.; Miravet, J. F.; Gavara, R.; Luis, S. V. *Chem.—Eur. J.* **2005**, *3*, 481–485; (b) Fuhrhop, J.-H.; Schnieder, P.; Rosenberg, J.; Boekema, E. *J. Am. Chem. Soc.* **1987**, *109*, 3387–3390.
19. (a) Brinksma, J.; Feringa, B. L.; Kellogg, R. M.; Vreeker, R.; Esch, J. v. *Langmuir* **2000**, *16*, 9249–9255; (b) Moniruzzaman, M.; Sundararajan, P. R. *Langmuir* **2005**, *21*, 3802–3807.
20. (a) Bychuk, O.; Shaughnessy, B. O. *Phys. Rev. Lett.* **1995**, *74*, 1795–1798; (b) Menger, F. M.; Yamasaki, Y.; Catlin, K. K.; Nishimi, T. *Angew. Chem., Int. Ed. Engl.* **1995**, *34*, 585–586.